UNIVERSITÀ POLITECNICA DELLE MARCHE

FACOLTÀ DI MEDICINA E CHIRURGIA

DOTTORATO DI RICERCA
in
SCIENZE BIOMEDICHE
XXX CICLO

ROLE OF THE Na^+/Ca^+ EXCHANGER 1 (NCX1) IN THE PROTECTIVE RESPONSE ELICITED BY GLUTAMATE IN CARDIAC CELLS EXPOSED TO HYPOXIA/REOXYGENATION (H/R)

Coordinatore:

Chiar.mo Prof. Salvatore Amoroso

Tutore:

Dr. Vincenzo Lariccia

Candidata:

Dott.ssa Marta Maiolino

Anno Accademico 2016/2017

INDEX

1. INTRODUCTION

Disorders characterized by ischemia/reperfusion (I/R), included myocardial infarction, stroke, and peripheral vascular disease, alone account for >12% of all deaths; more than HIV/AIDS, tuberculosis, lung and breast cancer together (Ferrer Gracia, Hernandez-Antolin et al. 2007). The World Health Organization (WHO) continues to emphasize the importance of cardiovascular diseases (CVDs) as a major cause of death in the Western world, with 30 to 50% of patients dying each year within a few hours of the onset of symptoms of acute myocardial infarction (AMI) (Herlitz, Dellborg et al. 2008). The majority of all CVD deaths (greater than 75 percent) are due to heart attacks and strokes. Growing evidence reports that mortality rates from CVD vary considerably between males and females and also between countries. In Europe, more than 4 million people die from CVD across every year, accounting for 45% of all deaths; 49% of deaths among women and 40% among men, with 1.4 million of these deaths before the age of 75 years. The 2016 Heart Disease and Stroke Statistics update of the American Heart Association (AHA) has reported that in the USA 15.5 million persons ≥20 years of age have CVD, whilst the reported prevalence increases with age for both women and men. Further, each year in the Western countries there are approximately 1 million of myocardial infarctions and 700,000 patients undergoing cardioplegic arrest for various cardiac surgery (Roger 2007). Minimizing ischemic time in both of these clinical scenarios has appropriately received a great deal of attention owing to the long-established relationship between duration of ischemia and the extent of myocardial injury. Once coronary flow is restored, however, the myocardium is susceptible to another form of insult stemming from reperfusion of the previously ischemic tissue (Kalogeris, Baines et al. 2012). Given that cardiac ischemia is either unpredictable (due to myocardial infarction) or inevitable (in the operating room), there is great interest in developing strategies to minimize reperfusion-mediated injury.

1.1 General features of myocardial I/R

Myocardial ischemia occurs for a mismatch between blood flow and metabolic requirements, when the rate of oxygen and metabolic substrates delivery to the heart is insufficient to meet the myocardial energy requirements. Restoration of oxygenated blood flow, although necessary to re-establish delivery of oxygen and nutrients to support cell metabolism, may induce pathogenic processes that exacerbate the ischemic injury, thus producing a further injury known as I/R injury. Thus, total injury sustained by a tissue represents the sum of damage attributable to ischemia *per se* plus that invoked by reperfusion, which can be manifested as myocardial necrosis, arrhythmia, myocardial stunning, endothelial and microvascular dysfunction including the no-reflow phenomenon (Kalogeris, Baines et al. 2012). The extent of the ischemic insult is determined primarily by the magnitude and duration of the interruption in the blood supply, whereas the subsequent damage induced by reperfusion is due to mediator release into the bloodstream draining revascularized tissues and subsequent delivery to remote organs. The mechanism of I/R is multifactorial and involves divergent biological pathways. I/R is responsible for endothelial activation leading to microvascular dysfunction and deterioration of coronary flow reserve (Ferguson, Smith et al. 1986, Taqueti and Ridker 2013), vasoconstriction and spasm (de Servi, Poma et al. 1988), myocardial contractile dysfunction (Weisel 1993), reperfusion arrhythmias(Anselmi, Abbate et al. 2004), activation of the inflammation cascade (cytokines, chemokines, complement activation, neutrophil activation) (Levy and Tanaka 2003, Merchant, Nadaraj et al. 2008) and coagulation imbalances (Raivio, Lassila et al. 2009). In summary, the restriction in blood flow to the heart and the following restoration of oxygen and substrates supply leads to cell damage which might result in the development of myocardial infarction, contractile dysfunction and arrhythmias. As a result of intensive investigation over decades, a detailed understanding of

the anatomic and biochemical substrates that contribute to the genesis of I/R injury have been well characterized (Kalogeris, Baines et al. 2012, Lejay, Fang et al. 2015).

1.2 Pathophysiology of myocardial ischemic injury

Myocardial ischemia results in a characteristic pattern of metabolic and ultrastructural changes that may lead to irreversible injury (**Fig. 1.1**). In absence of oxygen, mitochondrial oxidative phosphorylation rapidly stops leading to mitochondrial membrane depolarization, ATP depletion, and inhibition of myocardial contractile function (Kalogeris, Baines et al. 2012). This process is exacerbated by the breakdown of any available ATP, as the F1-F0 ATPase functions in reverse to maintain the mitochondrial membrane potential. A compensatory increase in anaerobic glycolysis for ATP production leads to the accumulation of hydrogen ions and lactate, resulting in intracellular acidosis (pH to <7.0) and inhibition of mitochondrial fatty acid and residual energy metabolism. Thus, the impaired ATP synthesis rate is the main cause of the imbalances in ionic state across cellular membranes, largely due to the inability of ATP-dependant pumps to function. In detail, at cellular level there is initially an increased K^+ efflux related to an increased osmotic load due to the accumulation of metabolites and inorganic phosphate. An increase in free Mg^{2+} is followed by a decrease in total Mg^{2+}. Then, a substantial decline in ATP leads to Na^+/K^+-ATPase inactivation, resulting in a further decline of K^+ and an increase in Na^+. The mechanisms underlying the increased Na^+ early in ischemia are failure to extrude Na^+ via the Na^+/K^+-ATPase and Na^+ influx via Na^+/H^+ exchange, Na^+-HCO^{3-} cotransport (NBC) and the voltage-gated Na^+ channel. Na^+ efflux via the Na^+/K^+-ATPase is attenuated during ischemia, therefore activation of other mechanisms leads to increased intracellular Na^+. Both the Na^+/H^+ exchanger and the cotransporter (NBC) might also contribute to Na^+ influx (Baetz, Bernard et al. 2003). In

response to the increased intracellular Na^+ concentration, the activation of the sodium/calcium exchanger (NCX), which will be discuss further in detail, in its reverse mode of operation results in intracellular Ca^{2+} overloading as the cell tries to extrude Na^+.

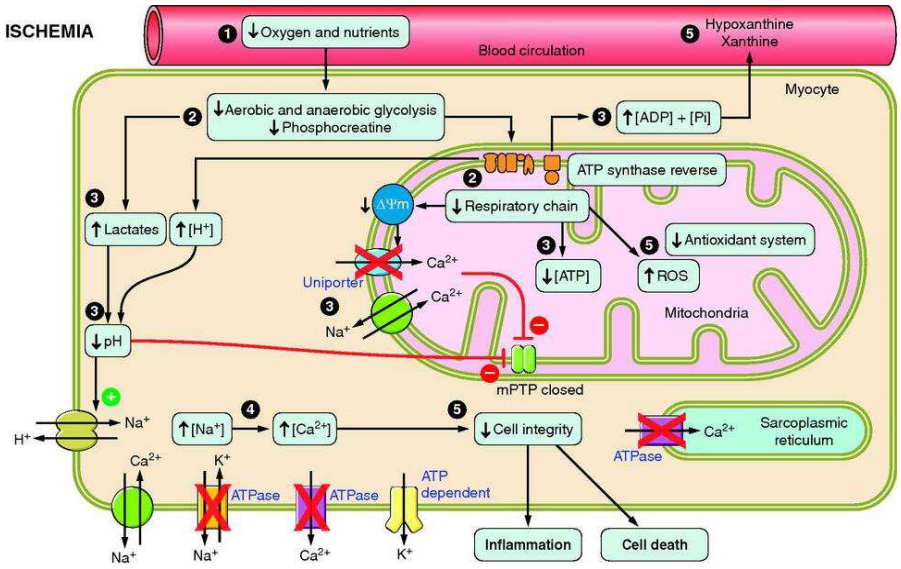

Fig. 1.1: Main events of ischemia injury. Ischemia decreases energy content, acidifies intra- and extracellular environments, and alters ionic homeostasis. Ca^{2+} accumulation and reactive oxygen species (ROS) production impair cell integrity (Paradis, Charles et al. 2016).

Moreover, in addition to disruptions in ionic homeostasis, cellular systems are overwhelmed by an increase in reactive oxygen species (ROS) production and oxidative stress, which can result in further defective Ca^{2+} handling (Tompkins, Burwell et al. 2006). More specifically free radicals can impair Ca^{2+} stimulated SR and sarcolemmal Ca^{2+} ATPase activity, thereby reducing calcium transport into the SR or out of the cell, and exacerbating Ca^{2+} overload within the ischemic cell (Netticadan, Temsah et al. 1999). The rise in cytosolic Ca^{2+} results in cellular damage by activation of Ca^{2+} dependent phospholipases, proteases, and calpains, causing further membrane swelling and rupture, in addition to ischemic contracture. In particular, activation of intracellular proteases (e.g., calpains) damages the myocardial interstitium and microvasculature by producing hypercontracture and contracture band

necrosis. The necrosis of myocytes and no myocytes triggers an inflammatory reaction with subsequent organization and healing (Casey, Arthur et al. 2007). The degree of tissue injury varies in extent with the magnitude of the decrease in the blood supply and with the duration of the ischemic period (Frank, Bonney et al. 2012).

1.3 Pathophysiology of myocardial reperfusion injury

Under experimental circumstances and in clinical situations, ischemia may be followed by reperfusion, that is, the readmission of oxygen and metabolic substrates with washout of ischemic metabolites. Although, reperfusion is essential to salvage ischemic tissue, it has the potential to cause further irreversible cell damage called as reperfusion injury (**Fig. 1.2**). Restoration of blood flow leads to increasing intracellular pH due to H^+ washout and inadequately restored ATP synthesis, Ca^{2+} overload and reduced contractility, coronary endothelial dysfunction, low production of nitric oxide and oxidative stress, migration of inflammatory cells, disruption of membranes and induction of apoptotic and necrotic signals in the myocardium (Garcia-Dorado, Ruiz-Meana et al. 2009). Clearly the recovery of pH, oxidative stress and Ca^{2+} overload can induce the abrupt opening of the mitochondrial permeability transition pore (mPTP), a large conductance pore in the inner mitochondrial membrane, which dissipates mitochondrial membrane potential and strongly contributes to myocardial hyper-contracture, apoptosis and necrosis. Opening of the mPTP leads to the release of the enzyme cytochrome c, a potent activator of the apoptotic pathways, and leads to the hydrolysis of ATP rather than synthesis. This causes a rapid decline in the intracellular ATP concentrations, which causes the disruption of ionic and metabolic homeostasis and activation of degradative enzymes and ultimately results in irreversible cell damage and necrotic death (Schriewer, Peek et al. ; Casey, Arthur et al. 2007).

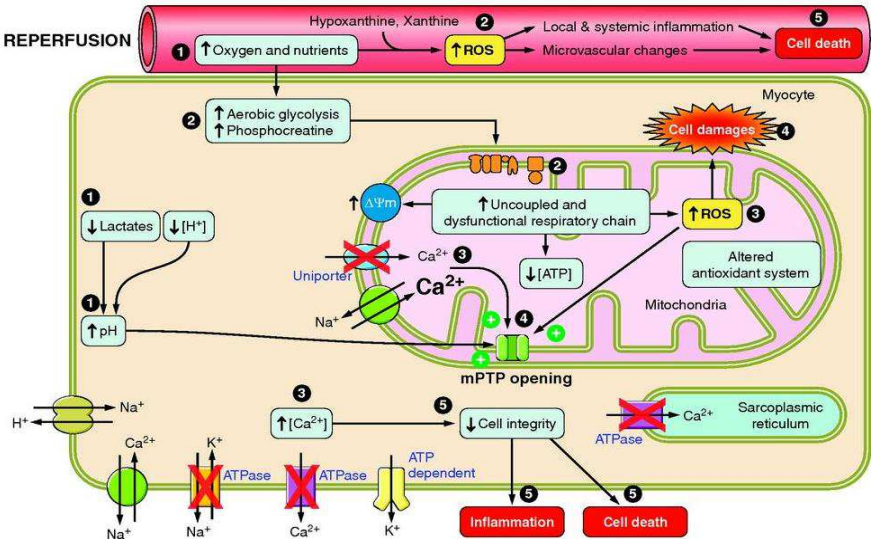

Fig. 1.2: Main events of reperfusion injury. Reperfusion restores pH, produces more ROS, and induces Ca^{2+} uptake, triggering inflammation, mitochondrial permeability transition pore (mPTP) opening, and cell death. ADP, adenosine diphosphate; ATP, adenosine triphosphate; Pi, inorganic phosphate; ΔΨm, membrane potential (Paradis, Charles et al. 2016).

The consequent Ca^{2+} increase also enhances ROS accumulation due to the activation of xanthine oxidase, NADPH oxidases, and mitochondria respiratory chain uncoupling (Yu, Lee et al. 2014), which further exacerbates membrane damage by directly promoting opening of the mPTP, and thus contribute to cell death during reperfusion (Perrelli, Pagliaro et al. 2011). The clinical outcome of reperfusion-mediated injury is also determined by a third phase of ROS production that occurs during post-reperfusion repair that is characterized by tissue remodelling and adaptation (Zorov, Juhaszova et al. 2006). Growing evidence suggests that a defect in myocardial Ca^{2+} transport system with consequent intracellular Ca^{2+} overload is one of the main contributors of myocardial I/R induced injury (Wei, Zhou et al. 2007).

1.4 Myocardial calcium handling

Ca^{2+} is a very essential intracellular messenger involved in many physiological processes, including muscle contraction, cell mobility, fertilization, exocytosis, and apoptosis. In cardiac

myocytes intracellular Ca^{2+} cycling can be understood as a balance between Ca^{2+} influx and efflux pathways governed by a dynamic network of physical and chemical signals. In physiological conditions, resting levels of cytosolic Ca2+ are maintained at submicromolar concentrations by three different mechanisms; (i) Limiting Ca^{2+} infiltration into the myocytes; (ii) Sequestering Ca^{2+} in the intracellular compartments; (iii) Extruding Ca^{2+} out of the cells against a 10 000-fold ionic gradient. Defined regulation of Ca^{2+} signals in the heart, which is crucial for the maintenance of the rhythmic contraction and force development, depend on the free intracellular Ca^{2+} level and the Ca^{2+} sensitivity of the cardiomyocytes. In cardiac cells Ca^{2+} ions are stored inside the SR, which can be utilized for fast contraction and other physiological activities. Calcium release from intracellular stores plays a central role in cardiac excitation–contraction (E-C) coupling (**Fig. 1.3**). During depolarization, a small amount of Ca^{2+} first enters through the L-type Ca^{2+} channel (LTCC), which are located in the membrane of T-tubules near the junctional region of the SR. This "calcium trigger" is thought to directly activate the calcium release channels driven in the junctional SR. Opening of these calcium-sensitive Ca^{2+} release channels known as ryanodine receptors (RyR) partially empties the internal store of calcium. This mechanism is known as calcium-induced Ca^{2+} release (Diaz, O'Neill et al. 2004). Binding of calcium to troponin C in the contractile apparatus initiates muscle contraction (systole), whereas calcium reuptake into the SR primarily by the phospholamban-regulated sarcoplasmic reticulum Ca2+-ATPase (SERCA) allows for cardiac relaxation (diastole). In normal hearts, sympathetic stimulation activates β1-adrenergic receptor, which in turn stimulates the production of cyclic cyclic adenosine monophosphate (cAMP) and thereby activates protein kinase A (PKA). PKA phosphorylates phospholamban and RyR, both of which contribute to an increased intracellular $[Ca^{2+}]i$ transient (Bers 2008).

1.4.1 Calcium overload during I/R

The pivotal role of calcium cycling and homeostasis has long been recognized in contractile, metabolic, electrical and ionic alterations associated with myocardial ischemia, as well as in hibernation, stunning and mitochondrial dysfunction associated with reperfusion. During ischemia, the ischemic tissues become dependent on anaerobic glycolysis for their ATP supply. This leads to an accumulation of lactate, protons, and NAD^+ which in turn causes a drop in cytosolic pH. In an attempt to re-establish normal pH, the cell extrudes H^+ ions in exchange for Na^+ via the plasmalemmal Na^+/H^+ exchanger (NHE) (Murphy and Allen 2009). Prolonged ischemia as well as reperfusion of ischemic heart cause intracellular Ca^{2+} overloading due to massive Ca^{2+} entry and dysfunction of Ca^{2+} sequestration mechanisms. Ca^{2+} infiltration during ischemia may predict the severity of Ca^{2+} influx during reperfusion leading to reperfusion-induced injury. This increase in cytosolic Ca^{2+} is greatly exacerbated upon reperfusion, where removal of extracellular H^+ ions further increases the proton gradient across the plasmalemma, thereby accelerating NHE exchanger function. In addition to detrimental alterations in plasmalemmal Ca^{2+} handling, the endoplasmic/sarcoplasmic reticulum (ER/SR) Ca^{2+} store is also affected during I/R. In particular, Ca^{2+} reuptake into the ER/SR by the SERCA ATPase is impaired by I/R, whereas Ca^{2+} release through the RyRs is enhanced (Netticadan, Temsah et al. 2000, Sanada, Komuro et al. 2011), both of which further exacerbate the lethal elevations in intracellular Ca^{2+}. Such dysregulation of Ca^{2+} homeostasis results in the alteration of a cascade of Ca^{2+}-dependent cellular events which are the characteristics of myocardial I/R injury (**Fig. 1.3**).

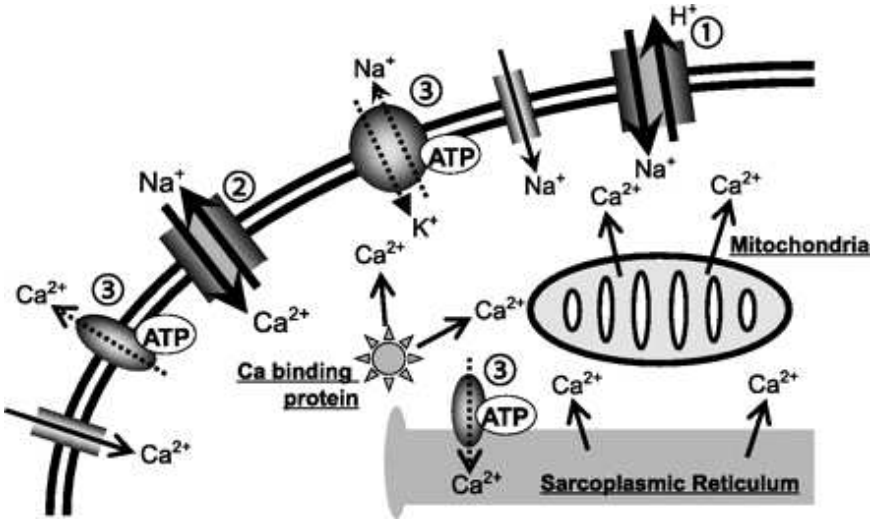

Fig. 1.4: Ion exchanges during ischemia: excretion of H+ due to pH lowering, deactivation due to loss of ATP, and reduction of Na^+/Ca^{2+} exchange due to lowered extracellular pH and intracellular accumulation of Na^+(Sanada, Komuro et al. 2011).

I/R-induced elevations in cytosolic Ca^{2+} leads to the pathological activation of Ca^{2+}/calmodulin-dependent protein kinases (CaMKs), which also contribute to cell death and organ dysfunction following ischemia. In addition, another target for Ca^{2+} are the calpains (Verburg, Murphy et al. 2009). This family of cysteine proteases is activated by elevation of Ca^{2+} and degrades a panoply of intracellular proteins, including cytoskeletal, ER, and mitochondrial proteins that predispose the myocyte to lethal reperfusion injury (Croall and Ersfeld 2007). One of the ways cells deal with this lethal increase in Ca^{2+} is to take it up into the mitochondria via the mitochondrial Ca^{2+} uniporter (MCU), a protein that uses the negative $\Delta\psi m$ to drive uptake of the positively charged Ca^{2+} ions into the matrix. However, if the elevations in mitochondrial Ca^{2+} become excessive, they can trigger the mPTP response (Tompkins, Burwell et al. 2006). Any major and chronic imbalance in Ca^{2+} handling, exceeding the physiological shifts in $[Ca^{2+}]i$, may result in gradual cellular $[Ca^{2+}]i$ overload, leading to highly increased arrhythmia propensity, or cell injury.

One of the key regulator in maintaining the balance of the intracellular Ca^{2+} is NCX, which plays an essential role in removal of Ca^{2+} in physiological conditions and also strongly

contributes to calcium overload during I/R. Since calcium overload is perhaps the most critical factor in determining the biochemical basis of ultimate myocytes cell death (Talukder, Zweier et al. 2009), the coordinated regulation of Ca^{2+} homeostasis through NCX need to be clearly understood in order to develop novel therapeutic strategies for patient care and for the prevention of I/R injury.

1.5 The sodium calcium exchanger (NCX)

NCX is a membrane associated protein that catalyses electrogenic exchange of 3 Na^{+} ions and 1 Ca^{2+} ion across the plasma membrane in a high capacity, and low Ca^{2+} affinity fashion. This transporter can operate in either the Ca^{2+} -efflux or Ca^{2+} -influx mode depending on the prevailing electrochemical driving forces of the substrate ions and the membrane potential. Three mammalian isoforms have been cloned to date (NCX1-3) and their splice variants are expressed in a tissue-specific manner (Philipson and Nicoll 2000, Lytton 2007) to fulfil physiological demands in excitable and non-excitable tissues (Carafoli 1987, Carafoli 1988, Blaustein and Lederer 1999) NCX2 and NCX3 have been found in the brain and skeletal muscle, whereas NCX1 is widely distributed in mammalian cells. The canine NCX1 subtype, which has been found to be predominantly expressed in the heart, was the first to be purified and cloned. The cardiac NCX consists of 970 amino acids with a molecular mass of 110 kDa. Biochemical analyses over the years have indicated the presence of 9 transmembrane segments (TMSs) (Ren and Philipson 2013). However, major advancement in understanding the structural basis has only recently been achieved by solving the crystal structure of a prokaryotic homologue of the exchanger, which revealed the presence of 10 α-helical TMSs rather than the 9 TMS proposed for NCX1 (Giladi, Lee et al. 2017). This model incorporates an additional TMS8 and an extracellular C-terminus (**Fig. 1.5**). Interestingly, NCX1 possess a

short motif (about 30 residues) that is similar to the Na^+/K^+-ATPase with residues 248–252 and 300–304 involved in its regulation by phospholemmon (Blaustein and Lederer 1999). The NH2-terminal portion of the loop has a 20-amino acid domain rich in hydrophobic and basic amino acids and is called the XIP (exchange inhibitor peptide) region. This region is associated with the sodium inactivation process and it can bind several peptide mimetic compounds. In this regard, recent research showed that a new cell penetrating peptide called P1 is capable to blocks the auto inhibitory XIP domain and enhances NCX activity (Molinaro, Pannaccione et al. 2015). Around the central zone of the loop in the NH2-terminal portion, there is a sequence of 135 amino acids containing highly acidic residues (two zones of three aspartyl each) that bind $[Ca^{2+}]i$ with high affinity; this region is responsible for the $[Ca^{2+}]i$-dependent or allosteric regulation of the exchanger (Matsuoka, Nicoll et al. 1995).

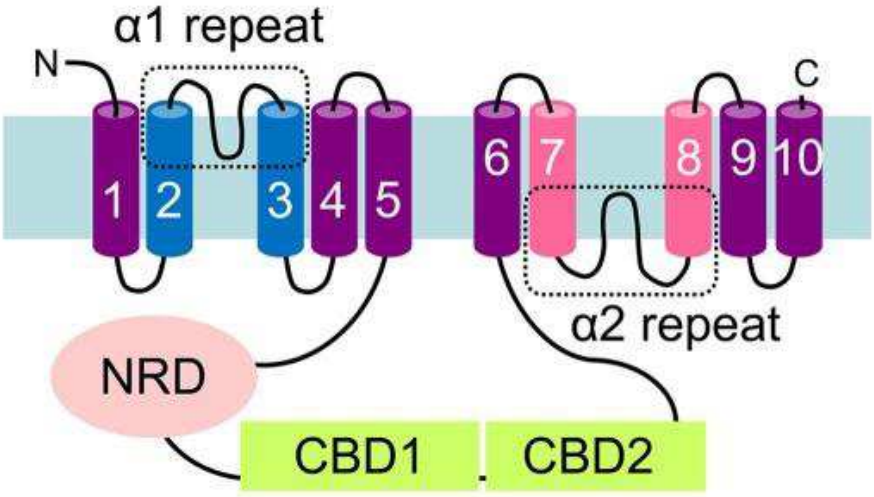

Fig. 1.5: The schematic molecular structure of NCX. The molecule contains 10 TM segments, a P-loop domain, and the second α repeat (α-2). The central regions of the two α repeats facing opposite in the membrane and contain amino acids that are essential for normal NCX function. The two CBD domains are different (CBD1,CBD2). CBD1 binds four Ca^{2+} ions with high affinity. CBD2 contains the variable alternative splicing region (Emery, Whelan et al. 2012) .

The properties of Ca^{2+}-binding proteins that participate in Ca^{2+}-dependent regulation of distinct cell-signalling pathways are controlled by tissue-specific expression and alternative

splicing of closely related genes. The isoform-dependent and alternative splicing-dependent modification of Ca^{2+}-binding regulatory domains are especially important for Ca^{2+}-transporting proteins operating in excitable tissues, since feedback interactions of Ca^{2+} with allosteric regulatory domains dynamically modulate the Ca^{2+}-transport rates in accordance with dynamic changes in cellular Ca^{2+} oscillations (Tal, Kozlovsky et al. 2016).

The differential role of NCX subtypes has been extensively investigated in ischemic renal and neuronal injury using various pharmacological tools as well as genetic models. The pathological role of NCX has been studied in I/R-induced renal injury using NCX1 heterozygous mice and it was observed that I/R-induced renal dysfunction, histological damage and Ca^{2+} accumulation in necrotic tubular epithelium were more markedly in NCX1 wild type than in NCX1 heterozygous mice (Yamashita, Kita et al. 2003). Some reports also supported the deleterious role of NCX revealing the efficacy of pre- and post-ischemic treatments with KB-R7943, an inhibitor of the reverse mode of NCX, which attenuate the I/R-induced renal injury by suppressing the intracellular Ca^{2+} overload (Yang, Jia et al. 2013, Yang, Jia et al. 2013). In the brain, unlike other tissues, NCX is present in the three different gene products NCX1, NCX2 and NCX3 with a distinct distribution pattern in different brain regions. Moreover, NCX subtypes may carry variable roles in ischemic injury and the mode of action of each subtype may vary in ischemia and reperfusion states exerting different roles during in vitro and in vivo anoxic conditions leading to a new paradigm in the pathogenesis of ischemic damage (Thurneysen, Nicoll et al. 2002). Thus, NCX subtype-specific strategies, which should be based on appropriate timing of administration, have become an alternative therapeutic approach to limit the severity of ischemic injury (Shenoda 2015). Indeed, the majority of in vivo studies using the focal cerebral ischaemia model indicate that blocking NCX activity is neurodamaging while increasing NCX activity is neuroprotective (Jeffs, Meloni et al. 2007, Sisalli, Secondo et al. 2014). More interestingly, this hypothesis was

supported by the observed increase in NCX1 and NCX3 activity responsible for Ca^{2+} cycling from ER and mitochondria leading to neuroprotection (Sisalli, Secondo et al. 2014). In this scenario, a promising selective compounds able to stimulate the activity of NCX1 and to prevent neuronal degeneration in vitro and in vivo models of ischemia has been recently synthesized (Molinaro, Cuomo et al. 2008). Over the last few years, although extensive studies have potentially revealed new molecular targets in cerebral ischemia, a thorough understanding of the role played by NCX still remains a controversial issue.

1.5.1 Role of NCX in myocardial I/R injury

In cardiac cells, NCX1 is one of the essential regulators of Ca^{2+} homeostasis playing an important role participating in nodal pace-maker activity (Groenke, Larson et al. 2013), cell metabolism (Magi, Lariccia et al. 2012, Magi, Arcangeli et al. 2013) and E-C coupling (Aronsen, Swift et al. 2013). In E-C coupling, contraction is initiated by influx of Ca^{2+} through voltage-dependent Ca^{2+} channels, which then triggers a release of Ca^{2+} from the SR by a Ca^{2+}-induced Ca^{2+} release mechanism. Relaxation is accomplished by the extrusion of Ca^{2+} from the cell by both NCX activity and by the reuptake of Ca^{2+} into the SR. In this scenario, the role of NCX as a primary Ca^{2+} extrusion mechanism in the heart is widely accepted. However, the expression and activities of NCX can be regulated by a variety of factors, among which, membrane potential, as well as Na^{+} and Ca^{2+} gradients, are crucial. NCX can be also a source for Ca^{2+}-influx, which can be enhanced by either decreasing the Na^{+} or increasing the Ca^{2+} gradients across the transarcolemmal membrane, bringing Ca^{2+} into cardiomyocytes in certain circumstances. Usually, the so called “reverse mode” of NCX becomes predominant in pathological settings, which can significantly alter Ca^{2+} homeostasis with output affecting numerous Ca^{2+}-dependent events that take place at the cellular or

systemic levels. During I/R, NCX acts reversely to induce Ca^{2+} influx, which strengthens Ca^{2+} overload that is mainly involved in cell structural damage, arrhythmia and systolic dysfunction (Bers 2008). Although ischemia and reperfusion are often referred to simultaneously, NCX may act differently during the ischemia and reperfusion phase. During ischemia, intracellular changes in Na^+ levels, pH and rigor shortening of the heart have been shown to be mediated by an increase in the Na^+/H^+ exchanger function. This leads to a rapid increase in intracellular Na^+ that alters the sarcolemmal Na^+ gradient, which in turn results in Ca^{2+} overload and swamping of the SR. In order to compensate, the NCX is upregulated to assist the SR in maintaining Ca^{2+} homoeostasis. However, following long periods of ischemia/hypoxia, reoxygenation of the cardiomyocytes, in which the cell tries to recover and re-establish the Na^+ and Ca^{2+} gradients, is not able to promote recovery (Chen and Li 2012). The role of NCX in cardiac cells following I/R has been largely investigated in different in vitro and in vivo models. Recent reports have shown that diabetic cardiomyocytes display an impaired $[Ca^{2+}]i$ homeostasis due to an altered NCX activity (Hattori, Matsuda et al. 2000, Ma, Zhu et al. 2008) that may precede clinically manifested cardiac dysfunction. Indeed, NCX protein levels as well as NCX activity during Ca^{2+} efflux have been found diminished in diabetic cardiac endothelial cells suggesting that the abnormal cardiac function might be due to the compromised ability to maintain Ca^{2+} homeostasis (Sheikh, Hurley et al. 2012).

Thus, the expression level and activity of NCX1 in the heart is an important factor in understanding cardiac pathophysiology. Other studies by using two different NCX1-KO mouse models revealed that the complete removal of the exchanger is associated with embryonic lethality, whereas its overexpression is linked to severe remodelling and heart failure. In particular, in heterozygous global NCX1-KO mice, with a 50% level of NCX1 expression, there are no significant structural as well as functional alterations of myocytes, whereas ventricular specific NCX1-KO mice, with NCX1 expression in only 10-20% of

myocytes, tolerate better I/R injury (Imahashi, Pott et al. 2005) but display cardiac alterations as animals age (Jordan, Henderson et al. 2010). Since the protein expression levels and/or regulation of NCX isoform/variants are disease related in many pathological states (e.g., heart failure, cardiac arrhythmia, and I/R injury), the selective pharmacological targeting of tissue-specific NCX variants could be beneficial, although this remains still a matter of debate (Giladi, Shor et al. 2016). The majority of studies often refers to a negative role of NCX during I/R, since a reduction of Ca^{2+} entry through its pharmacological or genetic inhibition would significantly limit the damage induced by I/R preventing the detrimental effect of Ca^{2+} overload (Weber, Piacentino et al. 2003, Imahashi, Pott et al. 2005). The lack of Ca^{2+} entry via the reverse-mode of NCX would decrease the detrimental effects of Ca^{2+} overload and better preserve ATP, which would prolong the activity of the Na^+/K^+-ATPase, leading to less Na^+ accumulation during ischemia in NCX-KO hearts. On reperfusion, the better-preserved ATP in the NCX-KO hearts facilitates Na^+ extrusion by Na^+/K^+-ATPase (Imahashi, Pott et al. 2005). Further, NCX mediates the increase in Ca^{2+}- CaMKII activity at the onset of reperfusion, which also increases the phosphorylation of Thr17 site of PLN, without changes in total protein, consistent with an increase in CaMKII activity. NCX inihibition produces a significant decrease in the phosphorylation of Thr17 of PLN with consequent decrease in infarct size, lactate dehydrogenase (LDH) release, and apoptosis produced by I/R injury. Taken together, these experiments indicate that the reverse NCX mode is a major pathway of Ca^{2+} influx upon reperfusion able to activate CaMKII which is considered a maladaptive mediator of cardiac ischemic injury (Salas, Valverde et al. 2010). Moreover, prior stimulation of the reverse-mode NCX not only reduces the infarct size but also attenuates arrhythmias induced by I/R (Zhang, Cheng et al. 2015, Castaldo, Macri et al. 2016). However, recent studies have demonstrated that NCX1 activity can be strategic for cardioprotection against I/R evoked by conditioning programs, whereby short periods of

subcritical ischemic stimuli confer protection. Collectively these findings confirm that NCX1 may have a deleterious role in I/R, but it may be also beneficial in promoting cardioprotection. Thus, up to date a dual role of NCX1 in cardiac ischemia is emerging: on the one hand its inhibition during I/R might lead to cell survival, on the other hand its activity can be strategic as a trigger for the induction of ischemic tolerance.

1.6 Cardioprotective strategies against I/R injury

The pathophysiology of ischemic heart disease is complex, and a therapeutic strategy capable of activating multiple arms of the cardioprotective signalling network and/or simultaneously counteracting multiple mediators of I/R injury would likely have the greatest efficacy in mitigating ischemic death. It is well known that the extent of cell dysfunction, injury, and/or death is influenced by both the magnitude and the duration of ischemia. In recognition of this fact, revascularization and restoration of blood flow as soon as possible remains one of the the mainstay of all current therapeutic approaches to ischemia (**Fig. 1.6**). Over the years, huge efforts have been made to ensure early reperfusion according to the "time is muscle" principle: the quicker the perfusion is restored, the more heart tissue is saved. In particular, if reperfusion is instituted within 2 to 3 h of the onset of ischemia, the amount of salvage greatly exceeds the amount of myocardium undergoing irreversible reperfusion injury. Prompt restoration of blood flow can lead to the conversion from reversible to irreversible injury of a population of myocytes that have been severely impaired during the prior period of ischemia. For that reason, the treatment of reperfusion injury following ischemia is primarily supportive, even though no specific target-oriented therapy has been validated so far (Garcia-Dorado, Rodriguez-Sinovas et al. 2014). Therefore, there is a great need for the development of novel ischemic heart disease therapies that can make the heart more

resistant to ischemic death, the so called "cardioprotective" interventions. Pharmacological, mechanical, and combined reperfusion techniques have been refined over the years, and their efficacy has been greatly advanced by the development of adjunctive therapies (Gerczuk and Kloner 2012) .

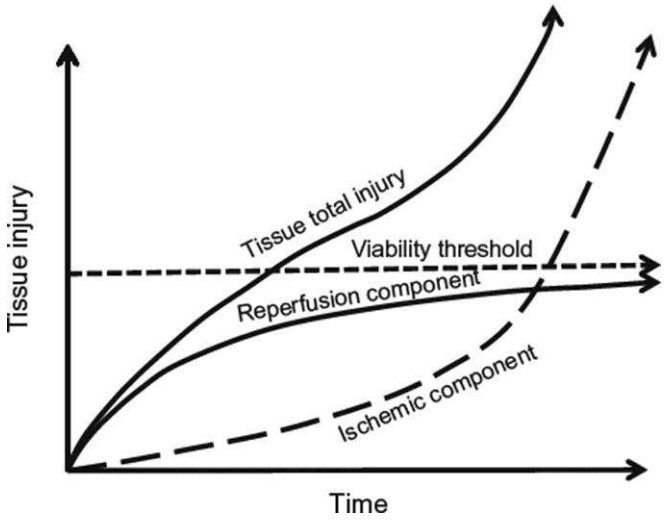

Fig. 1.6: Total injury sustained by a tissue subjected to I/R. Tissue injury and/or death occur as a result of the initial ischemic insult due to the magnitude and duration of the interruption in the blood supply, and then subsequent damage induced by reperfusion. Therapy against I/R injury will be more effective when administered after a period of ischemia that corresponds to the therapeutic window, where the major component of the total injury is due to reperfusion (Bulkley 1987).

Growing evidence has been shown that I/R-induced cell damage can be prevented or limited by triggering intrinsic adaptive response through non-pharmacological strategies such as ischemic pre-conditioning (PreC), ischemic post-conditioning (PostC) and hypothermia. Since 1986, the cardioprotective potential of conditioning programmes, whereby short periods of subcritical ischemic stimuli performed before (PreC) (Murry, Jennings et al. 1986) or after (PostC) (Vinten-Johansen and Shi 2011) the index ischemia, has been demonstrated by several reports. Intensive investigation of the mechanisms underlying PreC and PostC have identified a number of signal transduction pathways conveying the cardioprotective signal from the sarcolemma to the mitochondria, some of

which are overlapping. In fact, these pathways induce activation of signalling elements to preserve mitochondrial function during the early reperfusion following the index ischemia (Perrelli, Pagliaro et al. 2011). Another form of conditioning capable to increase myocardial salvage can be performed in a distant organ and it is known as "remote conditioning" (Healy, Feeley et al. 2015). Among these interventions, PreC has demonstrated the most consistent ability to confer robust cardioprotection in several different mammalian models (Cohen and Downey 1996). However, the clinical value of this approach is limited by the fact that patients suffering from myocardial ischemia do not present any symptoms until after the onset of ischemia. Among the non-pharmacological interventions, therapeutic hypothermia can also have a beneficial effect in limiting infarct size by lowering myocardial temperature during ischemia via reductions in metabolic demand, inflammatory response and platelet aggregation (Kanemoto, Matsubara et al. 2009). The fact that so many different interventions are capable of reducing ischemic death means that there are likely several pathways involved in the robust cardiac signalling network that can ultimately elicit a cardioprotective state. While the effects of myocardial ischemia on electrical propagation and stability have been studied in depth, the effects of I/R on energy metabolism has not been widely appreciated yet. Since changes in cardiac metabolism are understood to be an underlying component in almost all cardiac myopathies, the cardioprotective potential of interventions aimed to rescue the metabolic derangement occurring during I/R remains an active area of intense investigation. Thus, to optimize the heart's alternative fuel usage and minimize the I/R-induced damage, the molecular machinery involved in metabolic responses both in physiological and pathological conditions needs to be fully elucidated.

1.7 Myocardial energy metabolism

The heart is a highly active organ that consumes 10% of the body's total oxygen uptake and produces upwards of 35 kg of ATP every day (Taegtmeyer 1994). This high rate of energy flux required oxygen and a wide variety of metabolic substrates to supply the its vast energy needs.

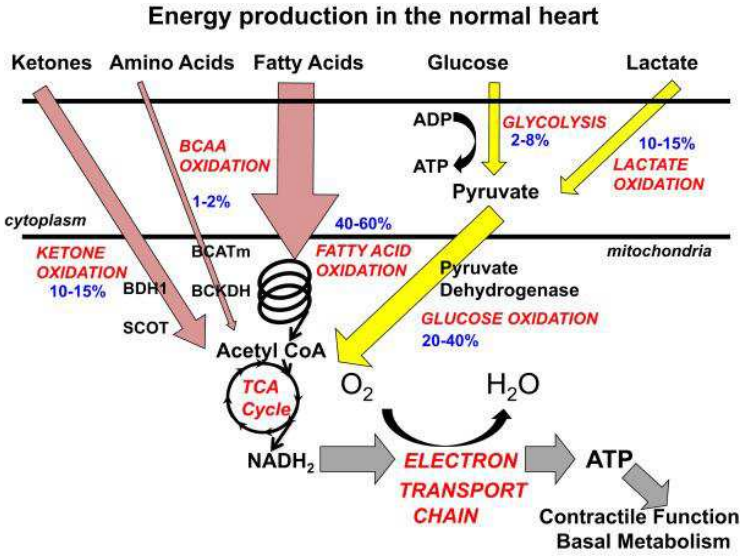

Fig. 1.7: Contribution of various metabolic pathways to energy production in the normal heart. ATP production in the heart originates primarily from the mitochondrial oxidation of fatty acids, pyruvate (originating from glucose and lactate), ketones, and amino acids (Lopaschuk 2017).

Central to the coordinated energy transduction function is the multi-purpose organelle mitochondrion, which occupies one third of the cell volume in cardiac myocytes making them the cell type with the highest mitochondria content. While a constant supply of substrates through the metabolic network is paramount for mitochondrial conversion of ATP, it is increasingly recognized that metabolites generated by both ATP-producing and non-ATP producing pathways can become critical regulators of cell function (Kolwicz, Purohit et al. 2013). In a normal heart, mitochondria are largely fueled by fatty acyl-CoA and pyruvate,

which are the primary metabolites of fatty acids and carbohydrates, respectively. The entry of long-chain acyl-CoA into the mitochondrion is a regulated process; with the rate-limiting step at the muscle form of the carnitine-palmitoyl transferase I (mCPT-1) reaction (Smith, Perry et al. 2012). The oxidation of pyruvate is regulated at the pyruvate dehydrogenase (PDH) reaction whereas other substrates, including lactate, ketone bodies and amino acids, can enter mitochondria directly for oxidation (McCommis, Chen et al. 2015, McCommis and Finck 2015). The contribution of ketone bodies and amino acids to overall cardiac oxidative metabolism, however, is considered to be minor due to the low availability of these substrates under normal physiological conditions. Metabolism of ketone bodies yields acetyl-CoA while amino acid catabolism yields keto-acids which are further metabolized to enter the TCA cycle (Kolwicz, Purohit et al. 2013) (**Fig. 1.7**). It is widely accepted that fatty acids are the predominant substrate utilized in the adult myocardium. However, the cardiac metabolic network is highly flexible in utilizing other substrates when they become abundantly available. For example, cardiac extraction and oxidation of lactate becomes predominant during exercise as skeletal muscle lactate production increases (Goodwin and Taegtmeyer 2000). The metabolic flexibility of the heart, which results in modulations of myocardial energetic and contractile function, confers the advantage of adequately supplying ATP under a variety of patophysiological conditions (Schaper, Meiser et al. 1985).

1.7.1 Energy metabolism impairment during I/R

In many types of heart diseases and dysfunctions, metabolism is the first area affected, which can then lead to channelopathies, ion imbalance, decreased contractile function, increased free radical production and cardiac death. Fortunately, the heart is also quite resilient, being able to maintain contractile function even under ischemic and anoxic

conditions. In this light, an understanding of metabolism is crucial for any study of the heart, which under conditions of prolonged stress or ischemia is capable of utilizing glucose, lactate, fatty acids, ketone bodies as alternative metabolic substrates (de Windt, Cox et al. 2002). It is well known that the heart's primary metabolic substrates under normal conditions are fatty acids and lactate, but under conditions unfavorable for oxidation, i.e., ischemia, anoxia and many types of cardiomyopathy, fatty acid oxidation is inhibited and the heart preferentially performs glycolysis and substrate-level phosphorylation. Without oxygen, the heart cannot break down fatty acids and ketone bodies into acetyl-CoA (Stanley 2004). There is also a decrease in fatty acid consumption and an increase in glycolysis in hypertrophied hearts.

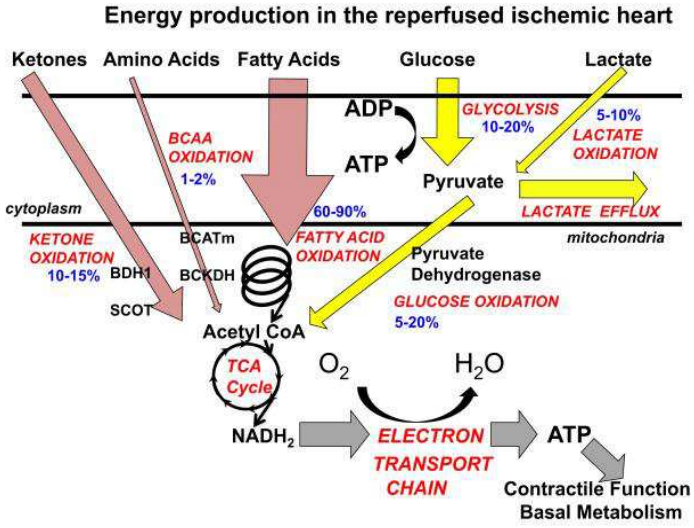

Fig. 1.8: Contribution of various metabolic pathways to energy production in the reperfused ischemic heart. During ischemia, ATP production decreases due to a limitation of oxygen supply and glycolysis increases in attempt to compensate for the decrease in mitochondrial oxidative metabolism. During reperfusion, fatty acid oxidation rapidly increases and dominates as a source of ATP production, glycolysis remains high during reperfusion, and pyruvate is shunted toward lactate production because of the decreased mitochondrial oxidation of pyruvate (Lopaschuk 2017).

Thus, glucose and glycolysis become the primary means of producing ATP, but this yields far less energy per molecule and produces two protons per molecule of glucose

consumed. This energy deficit and acidification increase become especially important during acute ischemia, as a lower pH inhibits glycolysis. The heart is unable to produce sufficient ATP through glycolysis, and it will be forced to turn to anaerobic, non-glycolytic fuels, such as amino acids, to utilize alternative metabolic that do not strictly require oxidation and do not require glycolytic conversion, which contributes to increased acidification (**Fig. 1.8**).

1.8 Role of amino acids in cardiac metabolism

Amino acids play a central role in cardiac metabolism. They can be readily metabolized into Krebs cycle intermediates; even though not all amino acids are metabolized equally in the heart (Lopaschuk and Ussher 2017). There are several different pathways by which amino acids can be used to supply cardiomyocytes with energy.

- Glutamate and α-ketoglutarate are readily interconvertible via transamination reaction. This reaction lead to an increase in Krebs cycle intermediates called anaplerosis and contributes to the maintenance of oxidative capacity (Tepavcevic, Milutinovic et al. 2015).
- Asparagine can serve as a means of exporting nitrogen from the cell, or it can be converted to aspartate.
- Aspartate can be transaminated to oxaloacetate, an other crucial regulator of levels of Krebs cycle (Drake, Sidorov et al. 2012).
- Alanine is usually transported out of the myocardium to remove amine groups from the working cell or it can also be transaminated to become pyruvate (Taegtmeyer, Peterson et al. 1977).

- Branched Chain Amino Acid (BCAAs) can be converted to acetyl-CoA, pyruvate or succinyl-CoA through different processes (Huang, Zhou et al. 2011).

However, in the fully functional heart, amino acid metabolism makes up a very small percentage of cardiac ATP production, but as the heart becomes oxygen-limited, they become more important as alternative fuel source (**Fig. 1.9**). In low/no-oxygen conditions, the heart will switch to anaerobic, non-glycolytic fuels, such as amino acids to meet its energy requirements. In this scenario, amino acids are now becoming more widely appreciated as cardioprotective substrates, due to their potential for non-oxidative metabolism and their low contribution to cellular acidification. Since amino acids are synthesized in a wide variety of pathways and reactions, some of them are more readily converted to metabolic intermediates than others.

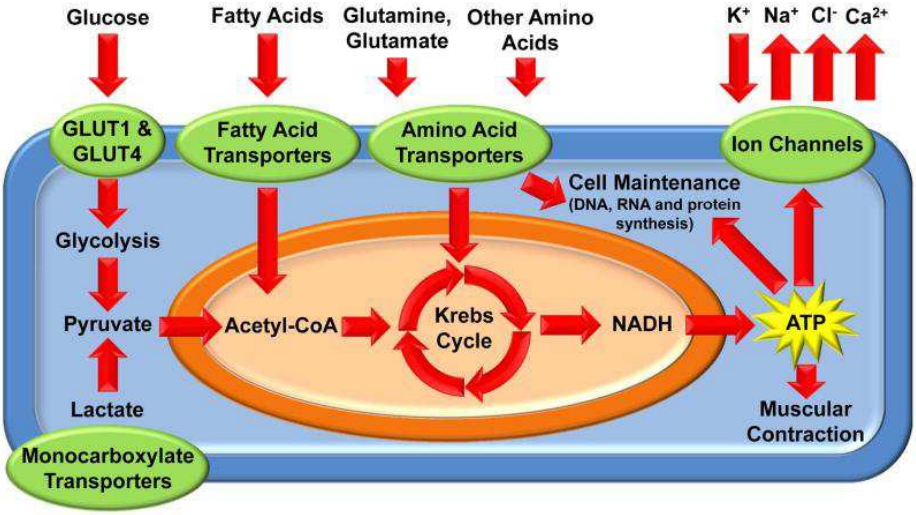

Fig. 1.9: Metabolite supply and function in the heart. The heart is capable of oxidizing a wide variety of substrates, including glucose, fatty acids and amino acids to supply its vast energy needs (Kolwicz, Purohit et al. 2013).

In particular, glutamate due to the ease with which this particular amino acid can be converted to α-ketoglutarate, may maintain the levels of Krebs cycle intermediates

keeping the metabolic machinery primed to begin oxidative phosphorylation as soon as oxygen returns improving the recovery after an ischemic event (Maus and Peters 2016).

1.8.1 Glutamate as metabolic substrate

Glutamate is classified as a non-essential amino acid, which means that it can be synthesized endogenously through distinct metabolic pathways (**Fig. 1.10**). In particular, It can be synthesized from glutamine, α-ketoglutarate and 5-oxoproline (Hu et al. 2010; Cho et al. 2001; Chen et al. 1998) and also serves as a precursor for the biosynthesis of amino acids such as L-proline and L-arginine (Young and Ajami 2000). Glutamate is also a neurotransmitter and may interfere with normal function of the nervous system, causing unintended side effects (Zhou and Danbolt 2014). However, also in the brain, glutamate may serve as an ideal metabolic substitute improving neurotoxic glutamate clearance and anaplerotic flux of TCA cycle intermediates in the stroke-affected brain (Khanna, Stewart et al. 2017, Rink, Gnyawali et al. 2017). In the brain, astrocytes, which are essential partners in neurotransmission, can readily shift the metabolic fate of glutamate removed from the synaptic cleft towards increased oxidative energy metabolism relative to direct formation of glutamine (Schousboe, Scafidi et al. 2014). In the heart, glutamate, which constitutes a major proportion of the free intracellular amino acid pool, is taken up in larger quantities than any other amino acid with an increased uptake during ischemia (Nielsen, Stottrup et al. 2011). Ischemia itself significantly reduces the tissue stores of glutamate, ATP and glutathione while increasing lactate levels (Wischmeyer, Jayakar et al. 2003). In response to ischemia, the heart will significantly enhance alanine production and glutamate consumption, though these effects become significant only when the partial pressure of oxygen in the tissue falls to 5% of normal levels (Peuhkurinen, Takala et al. 1983). During early post ischemic reperfusion myocardial glutamate concentrations

decrease in humans and in a rat isolated heart model (Kristiansen, Lofgren et al. 2008), likely due to an increased glutamate utilization. Numerous in vivo and in vitro studies have been conducted to delineate how glutamate can rescue cardiomyocytes from I/R-induced cell damage, in order to evaluate its potential as therapeutic tool. Indeed, isolation of cardiomyocytes in the presence of glutamate leads to an enhancement of their intracellular glutamate concentration. These glutamate-loaded cells exhibit a greater $NADH/NAD^+$ ratio, higher ATP levels and an enhanced capacity to remove intracellular reactive oxygen species during oxidative stress compared to control cells (Williams, King et al. 2001)

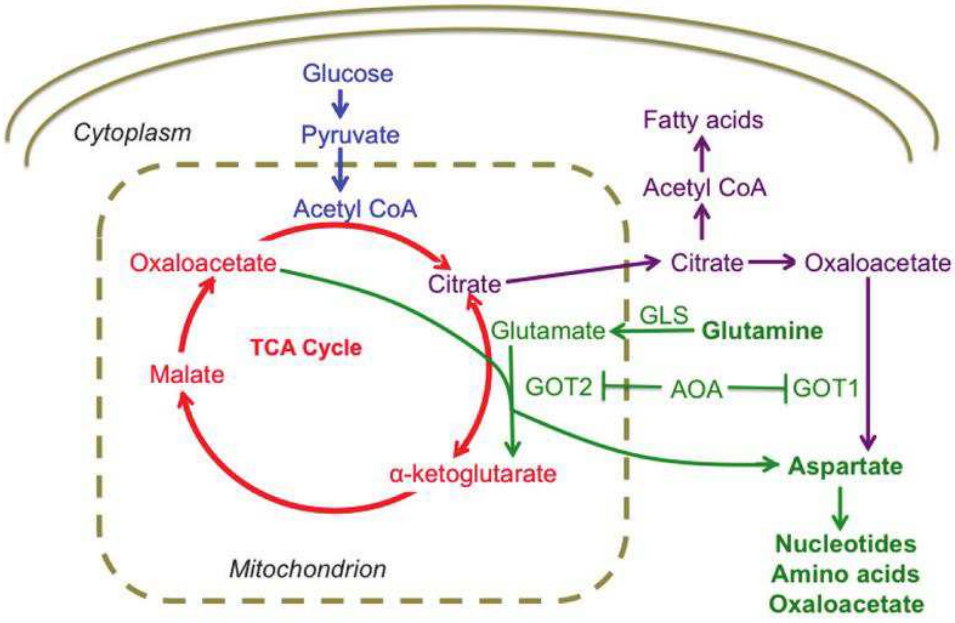

Fig. 1.10: Schematic overview of anaplerotic glutamate utilization as metabolic substrate. Glutamate derived from glutamine by glutaminase (GLS) is converted to α-ketoglutarate by glutamate oxaloacetate transaminase (GOT). Aminooxyacetate (AOA) inhibits GOT and therefore suppresses generation of α-ketoglutarate from glutamine-derived glutamate (Mukhopadhyay, Saqcena et al. 2015).

.Furthermore, exogenously administered glutamate given in the postoperative phase or as an adjunct to cardioplegic solutions reduces infarct size in patients with coronary artery disease and improves left ventricular recovery and function in patients undergoing

coronary artery bypass surgery (Svedjeholm, Vanhanen et al. 1996). These effects are likely depend on preserved transamination of glutamate and K-ATP channel activity (Kristiansen, Nielsen-Kudsk et al. 2005, Lofgren, Povlsen et al. 2010). The general idea is that glutamate may work as reservoir in cardiac output by maintaining metabolic intermediates acting as a substrate for complex I of the respiratory chain and/or as an intermediate for replenishment of citric acid cycle metabolites after ischemia and hypoxia (Drake, Sidorov et al. 2012).

Despite clinical and experimental evidence of a glutamate-induced cardioprotection in ischemia and other cardiac disorders, the underlying mechanisms for this effect has yet to be fully elucidated. The cardioprotective role of glutamate may stem from facilitation of cardiac cell function during anaerobic conditions as well as by supporting a rapid return to optimal function upon restoration of aerobic conditions. Both cases require the glutamate entry in to the cells and then into the mitochondria for enhancing activity-triggered metabolism. It is generally accepted that glutamate can get access to the mitochondrial matrix via the aspartate/glutamate carriers, a required component of the malate/aspartate shuttle (Wang, Chen et al. 2014). However, it has been recently proposed that glutamate may be carried in heart tissue through a family of proteins known as excitatory amino acid transporters (EAATs), which represent the major route of glutamate uptake into cells (Ralphe, Segar et al. 2004, King, Lin et al. 2006).

1.9 Excitatory amino acid transporters (EAATs)

The EAATs belong to the SLC1 family of transporters that also includes two mammalian neutral amino acid transporters as well as a large number of prokaryotic neutral and acidic amino acid transporters. There are five subtypes of EAATS, which are named EAAT1–5 in humans, with the rodent versions of EAAT1 and EAAT2 referred to as

GLAST1 and GLT1 respectively, and the rabbit version of EAAT3 referred to as EAAC1 (Vandenberg and Ryan 2013). Three of these transporters, EAAT1, EAAT3 and the variant form of EAAT2, are expressed in heart, with EAAT1 identified in the mitochondrial inner membrane, whilst EAAT2 and EAAT3 localise to the sarcolemmal membrane and T tubules (Shigeri, Seal et al. 2004). All EAATs are Na^+-dependent and display high affinity uptake of l-glutamate and d- or l-aspartate (**Fig. 1.11**). Limited data are available about the expression of glutamate transporters involved in the uptake of glutamate and in its role in the control of energy metabolism in cardiomyocytes. In this regard, an association of Glutamate–Aspartate Transporter (GLAST) (Karlsson, Tanaka et al. 2009), Glutamate Transporter 1 (GLT-1) (Genda, Jackson et al. 2011) and Excitatory Amino Acid Carrier 1 (EAAC1) (Magi, Lariccia et al. 2012) with glycolitic enzymes and mitochondria has been reported (Genda, Jackson et al. , Shigeri, Seal et al. 2004). Since EAATs transports glutamate using the favorable Na^+ gradient (Tzingounis and Wadiche 2007), their activity is expected to diminish as Na^+ accumulates, and eventually to stop unless specific mechanisms that preserve the Na^+ gradient are activated. The main Na^+ efflux system in the mitochondrial matrix in physiological conditions is the Na^+/H^+ exchanger (NHE), however its role in glutamate dependent influx pathway is presumably trifling, since H^+ is cotransported with Na^+ while glutamate is transported by EAATs (Vandenberg and Ryan 2013). Recent studies have suggested that the Na^+/K^+-ATPase, the antiporter enzyme which maintains the Na^+ and K^+ ion gradients across the membrane, may regulate glutamate uptake via EAATs (Wilmsdorff, Blaich et al. 2013). However, a variable but significant component of the Na^+ dependent glutamate transport activity is resistant to Na^+/K^+-ATPase inhibition, suggesting that the Na^+ gradient across the membrane may be sustained through a different mechanism (Rose, Koo et al. 2009).

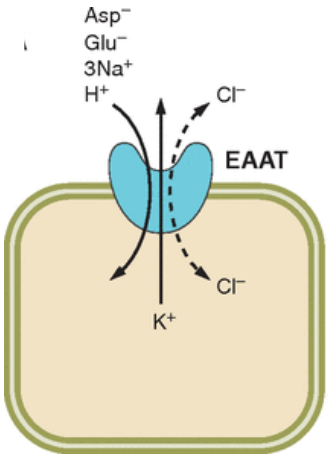

Fig. 1.11: Stechiometry of EAAT. Glutamate transport by the EAATs is coupled to the cotransport of 3 Na+ and 1 H+ followed by the countertransport of 1 K+ (Vandenberg and Ryan 2013).

1.10 NCX and EAATs interplay

Another transporter that may support glutamate entry via EAAT is NCX. It has been already proposed that glutamate and Na^+ entry via EAAT induces a Ca^{2+} response due to the reverse mode of plasma membrane NCX (Kirischuk, Kettenmann et al. 2007). However, our group for the first time showed a selective interaction between a specific EAAT subtype, EAAC1, and a specific NCX subtype, NCX1 at cytosolic and mitochondrial level. Their physical association, disclosed by their co-localization, coimmunoprecipitation and mutual activity dependency, emphasizes the high selectivity of the interaction, which represents a novel and complementary mechanism enhancing energy metabolism to meet the increased demand both in neuronal and cardiac model. The mitochondrial localization of EAAC1 and NCX1 suggests that such complex may represent another way by which glutamate enters into mitochondria to sustain energy production. According to this alternative pathway, EAAC1 and NCX1 exist as a macromolecular complex, which cooperate favoring glutamate entry into the cytoplasm and then into the mitochondria. The reverse mode of NCX activity allows glutamate entry

into the cells through EAAC1 leading to an increase in cytosolic [Ca^{2+}]. The increased ATP synthesis needed in many cells in which stimuli have increased cytoplasmic concentrations of calcium ions may be brought about, at least in part, by parallel increases in mitochondrial concentrations of calcium ions activating the intramitochondrial calcium-sensitive dehydrogenases (Denton 2009). The activation of these enzymes is important in the stimulation of the respiratory chain and hence ATP supply under conditions of increased ATP demand. This effect, in the presence of glutamate as substrate, may contribute to boost energy metabolism with a concomitant increase in ATP synthesis. Thus, the EAAC1-NCX1 dependent influx pathway, which play a crucial role in the glutamate-dependent metabolic response in physiological conditions (Magi, Lariccia et al. 2012, Magi, Arcangeli et al. 2013), may have important implications in I/R setting, where substantial changes in energy metabolism occur as a consequence of the reduced oxygen availability.

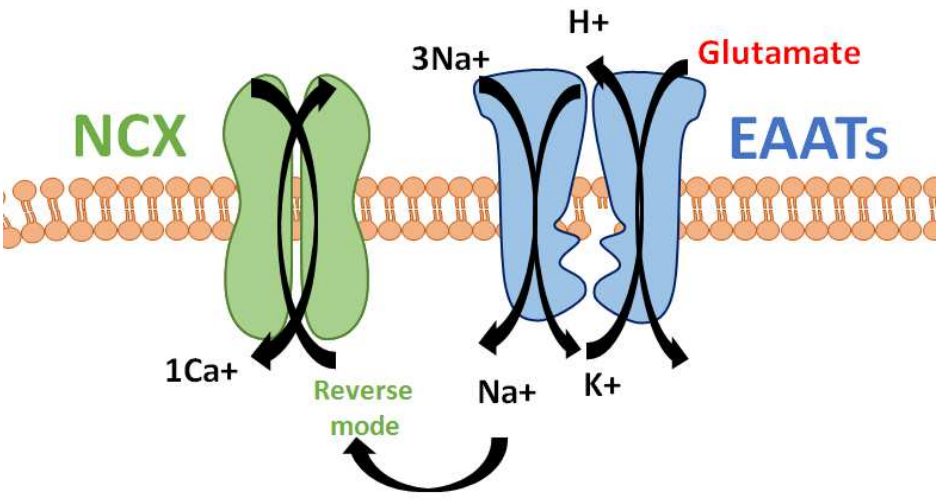

Fig. 1.11: Coordinated activity between NCX and EAATS. The reverse mode of NCX maintains the transmembrane Na^+ gradients, hence, supporting effective operation of glutamate uptake through EAATS.

1.11 Aim of the thesis:

On the basis of this previous finding, an experimental model of hypoxia/reoxigenation (H/R) has been employed in cardiac cells with the aim of:

- Investigating whether glutamate supplementation during the reoxygenation phase may improve the energy state of the cells and protect against H/R injury;
- Studying whether NCX and EAATs may be critically involved in the glutamate-induced metabolic response during H/R.

2. MATERIALS AND METHODS

2.1 Cell Culture

H9C2 rat cardiomyoblast, purchased from the American Type Culture Collection (CRL-1446), were used as in vitro model of cardiac myocites. Although H9C2 cells are no longer able to beat, they still show many similarities to primary cardiomyocytes, including membrane morphology, g-signalling protein expression and electrophysiological properties (Hescheler et al. 1991; Sipido and Marban 1991). For the experiments two different clones were used: H9c2 Wilde Type (WT), devoid of any detectable endogenous NCX1 and H9c2-NCX1 cells stably expressing NCX1 as previously described (Magi, Lariccia et al. 2012). Both cell lines were cultured as monolayer to sub-confluence in polystyrene dishes (100 mm diameter) and grown in Dulbecco's Modified Eagle Medium, DMEM (Invitrogen, Carlsbad, CA) supplemented with 10% heat inactivated fetal bovine serum (Invitrogen), 1% L-glutamine (200 mM) (Invitrogen), 1% sodium pyruvate (100 mM) (Invitrogen), 100 IU/ml penicillin (Invitrogen), and 100 μg/ml streptomycin (Invitrogen). Cells were grown in a humidified incubator at 37°C in a 5% CO2 atmosphere. Medium was changed every two days. Cells were plated the day before to conduct each experiment.

2.2 Isolation of rat adult ventricular cardiomyocytes

The animal experiments were conducted following the protocol approved by the Ethic Committee for Animal Experiments of the University Politecnica of Marche (Ref no. 721/2015-PR) and in strict accordance with the guidelines of the Italian Ministry of Health (D.L.116/92 and D.L.111/94- B). All efforts were made to minimize the number of animals used as well as their suffering.

Rat adult ventricular cardiomyocytes from one-month old male Wistar rats (Charles River, Lecco, Italy) were isolated by Collagenase type II-CLS2 (Worthington Biochemical Corporation, Lakewood, NJ) digestion using a modified Langendorff perfusion system. Firstly, rats were anesthetized with 4% isoflurane in 100% O_2 and then intraperitoneally injected with 1 ml of heparin (5000 IU/ml). After 10 min, the chest was opened and 1 ml of heparin (160 UI/ml) was injected into the right atrium. Then the heart was quickly excised, attached to the modified Langendorff perfusion system (**Fig. 2.1**) and retrogradely perfused with an O_2-saturated HEPES buffered solution containing (in mM): NaCl 140, KCl 4, HEPES 10, Na_2HPO4 0.5, $MgCl_2$ 1, $CaCl_2$ 1.5, glucose 15, pH 7.4 adjusted with NaOH

Figure 2.1: Fixation of the heart on Langendorff perfusion system.

After 2 min, the solution was switched to nominally Ca^{2+}-free HEPES buffered solution for 5 min, followed by perfusion with the same solution containing 100 µM EGTA for 2 min. After that, the heart was perfused with enzyme solution (150-200 U/ml) containing 30 µM blebbistatin (Sigma, Milan, Italy) until the heart became swollen and turned lightly pale (usually 10 min). The digestion was stopped by perfusing HEPES buffered solution containing 10% FBS. Perfusion solutions were constantly gassed with O_2 and the temperature was maintained at 37°C. The heart was then deprived of atria and aorta and put on a sterile

petri dish containing the perfusion solution without Ca^{2+}, with 100 μM EGTA and 30 μM blebbistatin. The ventricular tissue was chopped with small scissors, and single cells were isolated by mechanical dispersion. Single cardiomyocytes were harvested after filtration through a nylon mesh. At this point, Ca^{2+} was gradually reintroduced by incubating the cardiomyocytes in the perfusion solution with increasing concentrations of calcium, achieving a concentration of 1.8 mM as in the culture medium (O'Connell, Rodrigo et al. 2007). Once the cardiomyocytes were equilibrated (Ca^{2+} tolerant), they were plated at a density of 10 000 cells/cm2 on laminin coated dishes, and cultured in M-199 medium containing L-glutamine, NaHCO3 and Earle's salts, supplemented with 0.2% bovine serum albumin, 1X insulin-transferrin-selenium (Gibco, Grand island, NY, USA), 2 mM L-carnitine, 5 mM creatine, 3 mM taurine, 1% penicillin-streptomycin (Invitrogen), at 37°C in 5% CO2 atmosphere 38. The medium was prepared 2-3 hr prior to myocyte isolation in 2% CO2, 37 °C incubator with the caps loose. Incubate for 1-3 hr to allow myocyte attachment at a rate of about 80%. After attachment, the medium containing unattached myocytes and cell debris was gently aspirated off and fresh culture medium was added to the sides of the plates. After 24 hours cells were subjected to H/R and used for the experiments.

2.3 In vitro hypoxia/reoxigenation challenge (H/R)

The day before the H/R experiment, cells were plated in 6 multiwell plates (120,000 cells/well for H9C2 cells or 10,000 cells/cm^2 for cardiomyocytes). Hypoxia was induced in an airtight chamber in which O_2 was replaced with N_2 in a glucose-free Tyrode's solution containing (in mM): NaCl 137, KCl 2.7, $MgCl_2$ 1, $CaCl_2$ 1.8, NaH_2PO_4 0.2 and $NaHCO_3$ 10, pH 7.4. After closing all sealable connectors, the chamber was transferred to an incubator and the cells were subjected to hypoxia at 37 °C. Reoxygenation was initiated by opening the chamber and then replacing the glucose-free Tyrode's solution with fresh Tyrode's solution containing 5.5 mM

glucose. The cells were then maintained in the incubator under an atmosphere of 5% CO2, at 37°C. The experimental timeline of the H/R protocol in H9C2 (**a**) and in isolated rat cardiomyocytes (**b**) is shown in **Fig. 2.2.**

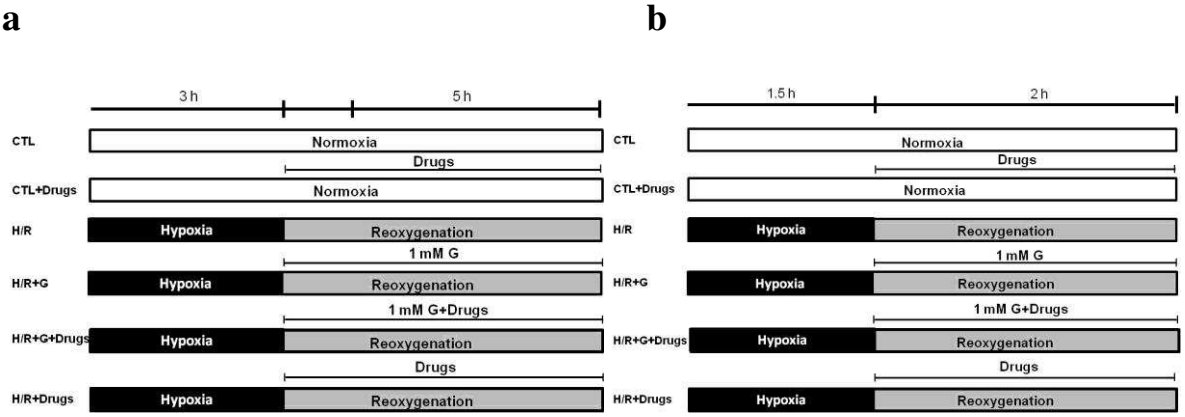

Fig. 2.2: Timeline of the experimental protocols (H/R). Schematic diagram showing the H/R timeline protocol in H9c2 cells (**a**) and in isolated rat adult cardiomyocytes (**b**). Control groups were incubated under normoxic conditions at 37 °C for the entire protocol. Glutamate (1 mM)-alone or in combination with 1 µM SN-6, 300 µM DL-TBOA or 3 µg/ml oligomycin (for ATP experiments conducted in H9c2-NCX1 cells)-was administered during the reoxygenation phase.

2.4 Determination of cell viability

2.4.1 LDH release assay

Cell injury induced by H/R protocol was quantified by measurement of lactate dehydrogenase (LDH) activity released from the cytosol of damaged cells in the experimental media. LDH is a soluble cytoplasmic enzyme that is present in almost all cells and is released into extracellular space when the plasma membrane is damaged. Cells were subjected to H/R protocol as described above (**Fig. 2.2**). At the end of the protocol, 100 µl of cell culture medium were removed and mixed with 100 µl of the reaction mixture (Diaphorase/NAD^+ mixture premixed with iodotetrazolium chloride/sodium lactate) in a 96 well plate. Then, the plate was incubated for 30 min at room temperature protected from light. After incubation,

LDH activity was assessed by reading the absorbance of the sample medium at 490 nm in a Victor Multilabel Counter plate reader (Perkin Elmer, Waltham, MA, USA).

2.4.2 FDA/PI double staining

For FDA/PI staining, H9c2 were plated on glass coverslips with a density of 120,000 cells/well and then subjected to H/R (**Fig. 2.2a**). At the end of the protocol, cells were treated with 36 μM FDA (Sigma) and 7 μM PI (Calbiochem., San Diego, CA, U.S.A.) for 10 min at 37°C in PBS. FDA once crossed the cell membrane is hydrolyzed by intracellular esterases producing a green-yellow fluorescence. If cells were damaged or dead FDA couldn't accumulate in cells. By contrast, PI is membrane impermeant and generally excluded from viable cells. Cell damage induced by H/R allows cell permeation by PI, which shifted its excitation maximum to the red by intercalating between the bases of DNA. Stained cells were examined immediately after the H/R protocol with an inverted Zeiss Axiovert 200 microscope (Carl Zeiss, Milan, Italy) and then analyzed. Excitation light was provided by an argon laser at 488 nm and emission wavelength was 510 nm and 625 nm for FDA and PI respectively.

2.5 Analysis of ATP production

The day before the experiment, cells were plated (5,000 cells/well) in 96 multiwell plates. For experiments conducted in normoxia, cells were first washed with Tyrode's solution containing (in mM): NaCl 137, KCl 2.7, $MgCl_2$ 1, $CaCl_2$ 1.8, NaH2PO_4 0.2, $NaHCO_3$ 10, glucose 5.5 mM, pH 7.4 and then exposed to different glutamate concentrations (0.5 and 1 mM) in the same Tyrode's solution for 1h at 37°C. For experiments conducted during H/R protocol, glutamate and the specific pharmacological tools were added in the same Tyrode's solution at the beginning of the reoxygenation phase and maintained for 1h. After the

incubation period, ATP levels were evaluated using a commercially available luciferase-luciferin system (ATPlite, Perkin Elmer, Waltham, MA) and protein content was determined by Bradford method with a luminescence counter (Victor Multilabel Counter, Perkin Elmer). Then, ATP levels were normalized to the respective protein content and expressed as nmol ATP/mg protein.

2.6 Bioenergetic analysis

The oxygen consumption rate (OCR), an indicator of mitochondrial respiration, and the extracellular acidification rate (ECAR), an indicator of glycolysis, were detected using the XF Cell Mito Stress Test and XF Glycolysis Stress Test by a Seahorse Bioscience XFp Extracellular Flux Analyzer (Seahorse Bioscience, USA). H9c2 cells (40,000 cells/well) were seeded on the XFp cell culture mini plates (Seahorse Bioscience, Billerica MA, USA) and subjected to the H/R challenge (**Fig. 2.2a**). At the end of the first hour of reoxygenation, the Tyrode's solution was replaced with 500 µl/well of XF24 running media. The plates were pre-incubated at 37 °C for 20 min in the XF Prep Station incubator (Seahorse Bioscience, Billerica MA, USA) in the absence of CO2 and then run on the XF24 analyzer to obtain OCR and ECAR. Several measures of mitochondrial respiration, including basal respiration, ATP-linked respiration, proton leak respiration and reserve capacity, were derived by the sequential addition of pharmacological agents to the respiring cells, as diagramed in **Fig. 2.3**. OCAR and ECAR were recorded during specified programmed time periods (three readings each) as the average numbers between the injections of inhibitors mentioned above. The final data calculation was performed after the readings and then normalized for total protein/well.

2.6.1 Oxygen consumption rate (OCR)

For the analyses of (OCR), as indicator of oxidative phosporilation, several parameters of mitochondrial respiration were measured before and after the addition of pharmacological inhibitors (**Fig. 2.3**). Initially, baseline cellular OCR is measured, from which basal respiration can be derived by subtracting non-mitochondrial respiration. Next oligomycin, a complex V inhibitor used to prevent the ATP-consuming reverse activity of ATP synthase, which may lead to cellular metabolic dysfunction and death, is added. The resulting OCR is used to derive ATP-linked respiration (by subtracting the oligomycin rate from baseline cellular OCR) and proton leak respiration (by subtracting non-mitochondrial respiration from the oligomycin rate). Next carbonyl cyanide-p-trifluoromethox- yphenyl-hydrazon (FCCP), a protonophore, is added to collapse the inner membrane gradient, allowing the ETC to function at its maximal rate, and maximal respiratory capacity is derived by subtracting non-mitochondrial respiration from the FCCP rate. Lastly, antimycin A and rotenone, inhibitors of complex III and I respectively, are added to shut down ETC function, revealing the non-mitochondrial respiration.

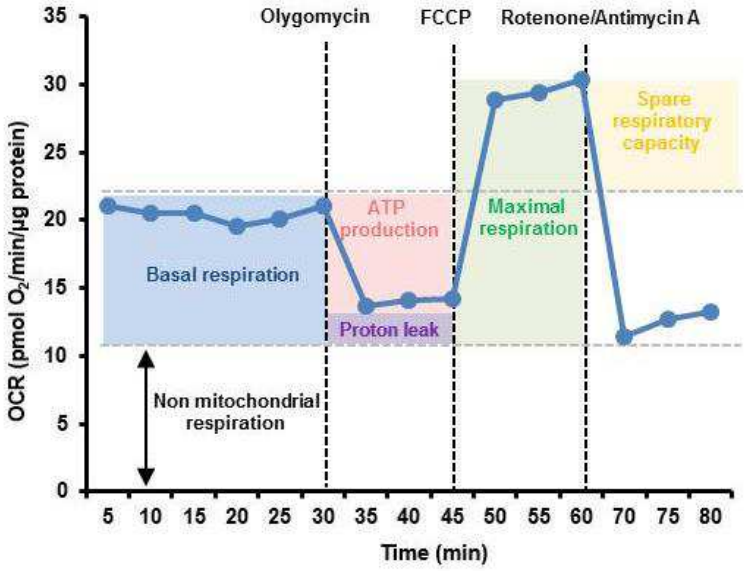

Figure 2.3: General scheme of mitochondrial stress test. Oligomycin (1.5 µM), FCCP (2 µM) and rotenone/antimycin A (0.5 µM) were sequentially introduced to measure basal

respiration, ATP production, proton leak, maximal respiration, spare respiratory capacity, and non-mitochondrial respiration.

Spare respiratory capacity is calculated by subtracting basal respiration from maximal respiratory capacity. A cell with a larger spare respiratory capacity can produce more ATP to maintain adequate levels of energetic molecules and overcome more stress.

2.6.2 Extracellular consumption acidification rate (ECAR)

ECAR is primarily a measure of lactate production and can be equated to the glycolytic rate (i.e., glycolysis). ECAR parameters were measured simultaneously with OCR in the Seahorse assay before and after the addition of pharmacological inhibitors, as shown by the general scheme in **Fig. 2.4**.

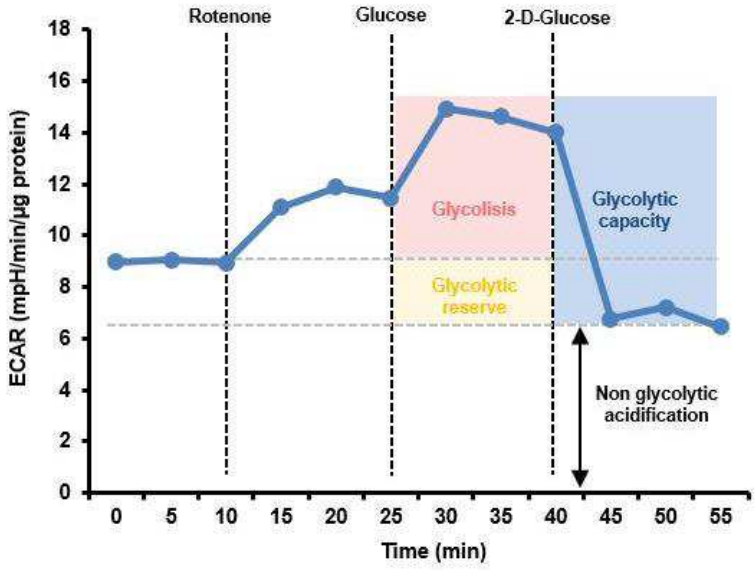

Figure 2.4: General scheme of glycolitic stress test. Sequential injections of rotenone (3 µM) glucose (10 mM), and 2-DG (100 mM) were used to measure glycolysis, glycolytic capacity and allow estimation of glycolytic reserve and non-glycolytic acidification.

Initially, rotenone was added to block complex I, thereby eliminating mitochondrial respiration and force cells to rely on glycolysis. Then sequential injections of glucose and 2-

deoxyglucose (2-DG), a glucose analog and inhibitor of glycolytic ATP production, were used to measure glycolysis, glycolytic capacity and allow estimation of glycolytic reserve and non-glycolytic acidification.

2.7 ROS detection

ROS production was assessed by using the cell-permeative probe 2′7′-dichlorodihydrofluorescein diacetate5 (H2DCFDA, Calbiochem, Vimodrone, Italy). This indicator is a no polar dye, converted into the polar derivative (H2DCF) by cellular esterases that are no fluorescent but switched to a highly fluorescent compound, 2′7′-dichlorofluorescein (DCF) when oxidized by intracellular ROS and other peroxides (**Fig. 2.5**) Upon stimulation, the resultant production of ROS causes an increase in fluorescence signal over time.

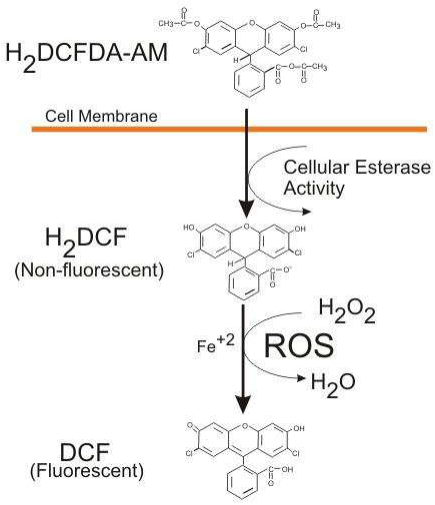

Fig. 2.5: Formation of fluorescent compound DCF by ROS. The acetate ester form of H2DCFDA-AM once inside the cell form the non-fluorescent moiety H2DCFDA, which is ionic in nature and therefore trapped inside the cell. Oxidation of H2DCFDA by ROS converts the molecule to DCF, which is highly fluorescent.

Briefly, H9c2 cells were plated in 12 multiwell plates and subjected to the H/R challenge. At the end of the protocol, cells were incubated in the dark for 30 min with 20 μM H2DCFDA.

Cells were subsequently washed twice with PBS and DCF fluorescence was measured using a multilabel microplate reader (Victor Multilabel Counter, Perkin Elmer) at excitation and emission wavelengths of 485 and 535 nm, respectively.

2.8 Western blotting

Cells were subjected to H/R protocol and then lysed using a protein lysis buffer containing (in mM): NaCl 150; Tris-HCl (pH 7.4), EDTA 10 (pH 8.0), SDS 1%, and a protease inhibitor cocktail mixture (Roche Diagnostics). Then, equal protein samples (50 µg, determined by Bradford method) were prepared in Laemmli buffer followed by boiling at 95°C for 5 min and subjected to SDS-PAGE as shown in **Fig. 2.6**.

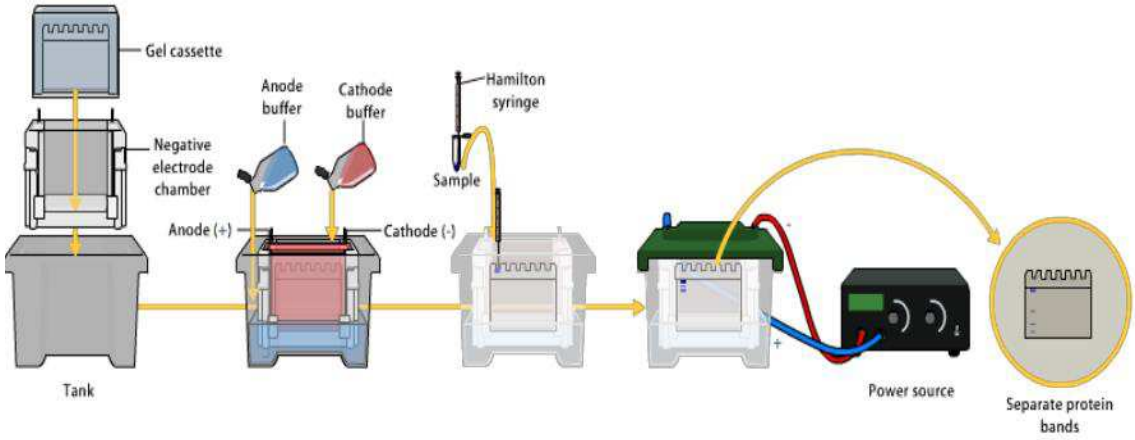

Fig. 2.6: Separation of proteins by SDS-PAGE. SDS. Equal amount of protein samples are loaded into a gel made of polyacrylamide and then an electric field is applied to the gel. The electric field acts as the driving force, drawing the SDS coated proteins towards the anode with larger proteins moving more slowly than small proteins. SDS-coated proteins are thus separated.

In this system, proteins denatured in the presence of SDS and 2-mercaptoethanol as thiol reducing agent acquired a rod-like shape and a uniform charge-to-mass ratio proportional to their molecular weights. The gels were stained with colloidal Coomassie stain and the protein sizes were determined by comparing the migration of the protein band to a molecular mass

standard (PageRuler prestained Marker, Fermentas). Proteins were transferred from the SDS gel onto polyvinylidine difluoride (PVDF) membranes as shown in **Fig. 2.7** (Immobilon Transfer Membranes, Millipore Co., Bedford, MA, USA) for 90 min at 200 mA using SD Semi-dry Transblot Apparatus (Bio-Rad). Then, the membrane was quickly rinsed with distilled H2O and protein bands detected with a Ponceau-S stain. After washing twice with H2O, the membrane was incubated with gentle agitation throughout all steps. After bathing in blocking buffer for 1 h at RT to reduce unspecific binding, the membrane was incubated with the appropriate primary antibody overnight at 4°. The day after, the membranes were washed (two quick washings followed by two washings with 5 min incubation) with TBS-Tween (0.5%) and incubated with the appropriate secondary antibody diluted in blocking buffer for 1 h at RT. After each antibody incubation step, the membrane was washed 4 times with PBS containing 0.1 % Tween 20 for 5 minutes. All incubation steps were performed under gentle shaking.

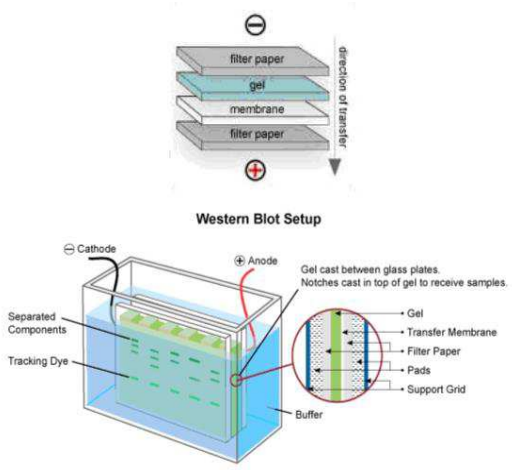

Fig. 2.7: Western Blot setup. Once the gel run is completed, gel is carefully removed from the plate and soaked in western blot transfer buffer. Then, electric current is applied to transfer the protein from the gel to the membrane.

The reactive bands were visualized employing a chemiluminescent reaction by incubation of the membrane (1 minute) with a 1:1 mixture of ECL solution A and B (Amersham

biosciences) as shown in **Fig. 2.8**. The enzyme horseradish peroxidase (HRP), which is coupled to the secondary antibodies, catalyzes the oxidation of luminol in the presence of H2O2. This chemical reaction results in the release of energy in the form of light. Finally, images were captured and stored on a ChemiDoc station (BioRad, Milan, Italy) and band densities were analyzed with the Quantity One (Bio-Rad) analysis software and normalized to β-actin, used as loading control.

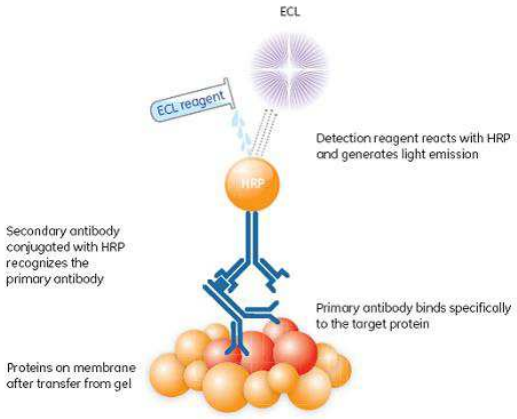

Fig.2.8: ECL protein detection. In the ECL systems, the enzyme horseradish peroxidase (HRP) conjugated to a secondary antibody is utilized to convert the substrate, producing light. The emitted light can be captured on an a ChemiDoc station (modified from gelifescience website).

2.8.1 Antibodies

Immunoblots were probed with the following primary antibodies:

- Anti-NCX1 IgG antibody produced in mouse was purchased from Swant, Bellinzona, Switzerland, (R3F1) and used at dilution 1:500.
- Anti-EAAC1 antibody produced in mouse was purchased from Chemicon International, CA, USA (AB1520) and used at dilution 1:1000.
- Anti-GLAST and anti-GLT14 produced in rabbit were both purchased from Alpha Diagnostic International and used at 1:1000 dilution.

- Anti-β-Actin antibody produced in mouse was purchased from Sigma (A5316) and used at diluition 1:1000.

2.9 Real-time confocal imaging

The day before the experiment H9c2-NCX1 cells were cultured on 25 mm coverslip. Afterwards, cells were subjected to H/R protocol and then loaded with the calcium indicator Fluo-4/AM (4 μM) for 30 min in the dark at room temperature (Molecular Probe, Eugene, OR), in a standard solution containing (inmM): NaCl 140, KCl 5, MgCl2 1, CaCl2 2, glucose 10, HEPES 20, pH 7.4 adjusted with NaOH. At the end of the Fluo-4/AM loading period, cells were washed and left in the standard solution for further 10 min to allow the complete de-esterification of the dye. Then the coverslips were placed into a perfusion chamber mounted onto the stage of an inverted Zeiss Axiovert 200 microscope. Real-time confocal imaging was used to evaluate NCX activity.

2.9.1 Analysis of NCX1 activity

NCX1 activity was evaluated as Ca^{2+} uptake through the reverse mode by switching the standard solution to a Na^{+}-free solution containing (in mM): LiCl 140, KCl 5, $MgCl_2$ 1, $CaCl_2$ 2, glucose 10, HEPES 20, pH 7.4 adjusted with LiOH. $[Ca^{2+}]i$ was measured by single-cell computer-assisted videoimaging using a LSM 510 confocal system (Carl Zeiss). Cells were treated according to the protocol schemes reported in **Fig. 1**. In particular, cells were exposed to glutamate and/or transporter inhibitors only during the reoxygenation phase or, for sham-treated cells (not subjected to hypoxia), under normoxia for equivalent length of time, and were not included in solutions used for Fluo-4/AM loading or fluorescence monitoring. Excitation light was provided by an argon laser at 488 nm and the emission was time-lapse

recorded at 505-530 nm. Images were acquired every 5s. Analysis of fluorescence intensity was performed off-line after images acquisition. Fluorescence intensity was expressed as F/F0-ratio, where F is the background subtracted fluorescence intensity and F0 is the background subtracted mean fluorescence value measured from each cell at resting conditions (F/F0). The NCX1 reverse mode activity was expressed as percentage of resting condition (Δ%) after H/R protocol. For Δ% calculation the maximal value of fluorescence obtained after stimulation was used and, as baseline, the mean of fluorescence recorded during the 30 seconds preceding the Na^+-free challenge.

2.10 Drug and chemicals

SN-6 and DL-TBOA were obtained from Tocris. All the other chemicals were of analytical grade and were purchased from Sigma.

2.11 Data processing and statistic

Data were expressed as mean ± S.E.M. Values less than 0.05 were considered to be significant. Differences among means were assessed by Student's t-test or one-way ANOVA followed by Dunnet's post hoc test. Statistical comparisons were carried out using the GraphPad Prism 5 software (GraphPad Software Inc., San Diego, CA).

3. RESULTS

3.1 Effect of glutamate on H/R injury: involvement of NCX1

First of all, an experimental model based on two H9c2 clones, H9c2-WT (not expressing endogenous NCX1 under our culture conditions) and H9c2-NCX1 (generated from H9c2-WT and stably expressing canine NCX1) was employed with the aim to explore the role of NCX1 in the glutamate effect on H/R injury. To this purpose, cells were subjected to 3 h of hypoxia followed by 5 h of reoxigenation as described in the protocol shown in **Fig. 2.2a** and then cell viability was assessed by analyses of extracellular LDH levels and fluorescein diacetate/propidium iodide (FDA/PI) double staining. As shown in **Fig 3.1** cell survival after H/R was significantly reduced in both H9c2 cell lines compared to their respective normoxic controls.

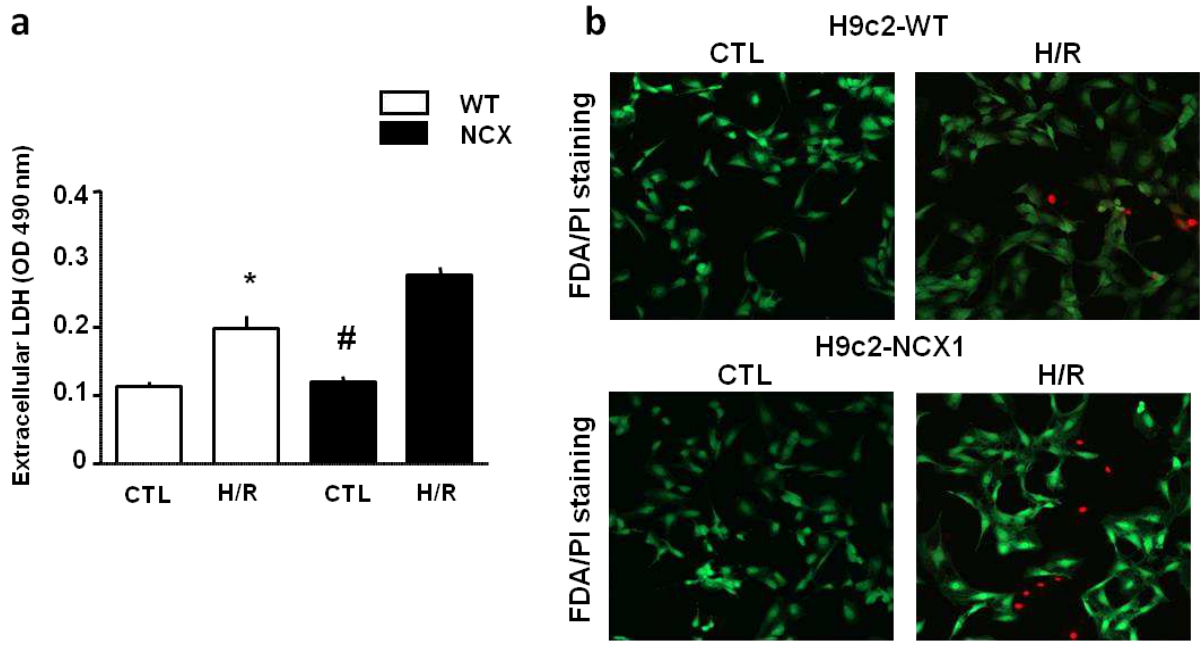

Fig. 3.1: Effect of H/R injury on cell survival in H9c2 cells. (**a**) Extracellular LDH activity measured 5 h after the hypoxic insult (3 h) both in H9c2-WT and in H9c2-NCX1 cells. Differences among means were assessed by one-way ANOVA followed by Dunnet's post hoc test. Each column represents the mean ± S.E.M. of almost 6 independent experiments performed in duplicate. *p<0.001 versus any other group; #p<0.001 versus H/R-WT group. (**b**) Evaluation of H9c2 survival by PI/F assay

showing the intravital staining that yields green-yellow fluorescence (FDA) for vital cells, and red fluorescence (PI) for dead cells, under normoxic (CTL) and H/R conditions. Red death cells tend to detach; thus images could underestimate their exact number. Images are representative of 3 independent experiments.

Secondly, to study the effect of glutamate on H/R injury and assess the specific contribution of NCX1, H9c2 cells were treated with glutamate at the onset of the reoxigenation and then cell viability was evaluated. Although H9c2-NCX1 cells are even more susceptible to H/R than H9c2-WT, as previously reported (Castaldo, Macri et al. 2016), glutamate supplementation during the reoxygenation phase fully prevented H/R injury only in H9c2-NCX1 but not in H9c2-WT cells (**Fig. 3.2b**). Notably, glutamate at the concentration used (1 mM) was devoid of detectable toxicity under normoxic conditions (**Fig. 3.2a**). Further evidence that a functional NCX1 is determinant for glutamate protection was obtained by evaluating the efficacy of glutamate to limit H/R injury after pharmacological blockade of NCX1. In particular, when H9c2-NCX1 cells were exposed to the selective NCX inhibitor 2-[[4-[(4Nitrophenyl) methoxy] phenyl] methyl]-4-thiazolidinecarboxylic acid ethyl ester (SN-6) (Niu, Watanabe et al. 2007) (1 μM) during the reoxygenation phase, glutamate was wholly ineffective in protecting cells from H/R injury (**Figs. 3.2a and c**). SN-6 *per se* has no effect on H9c2-NCX1 cell viability under normoxia or when introduced only at the reperfusion during our H/R protocol (**Figs. 3.2a and c**).

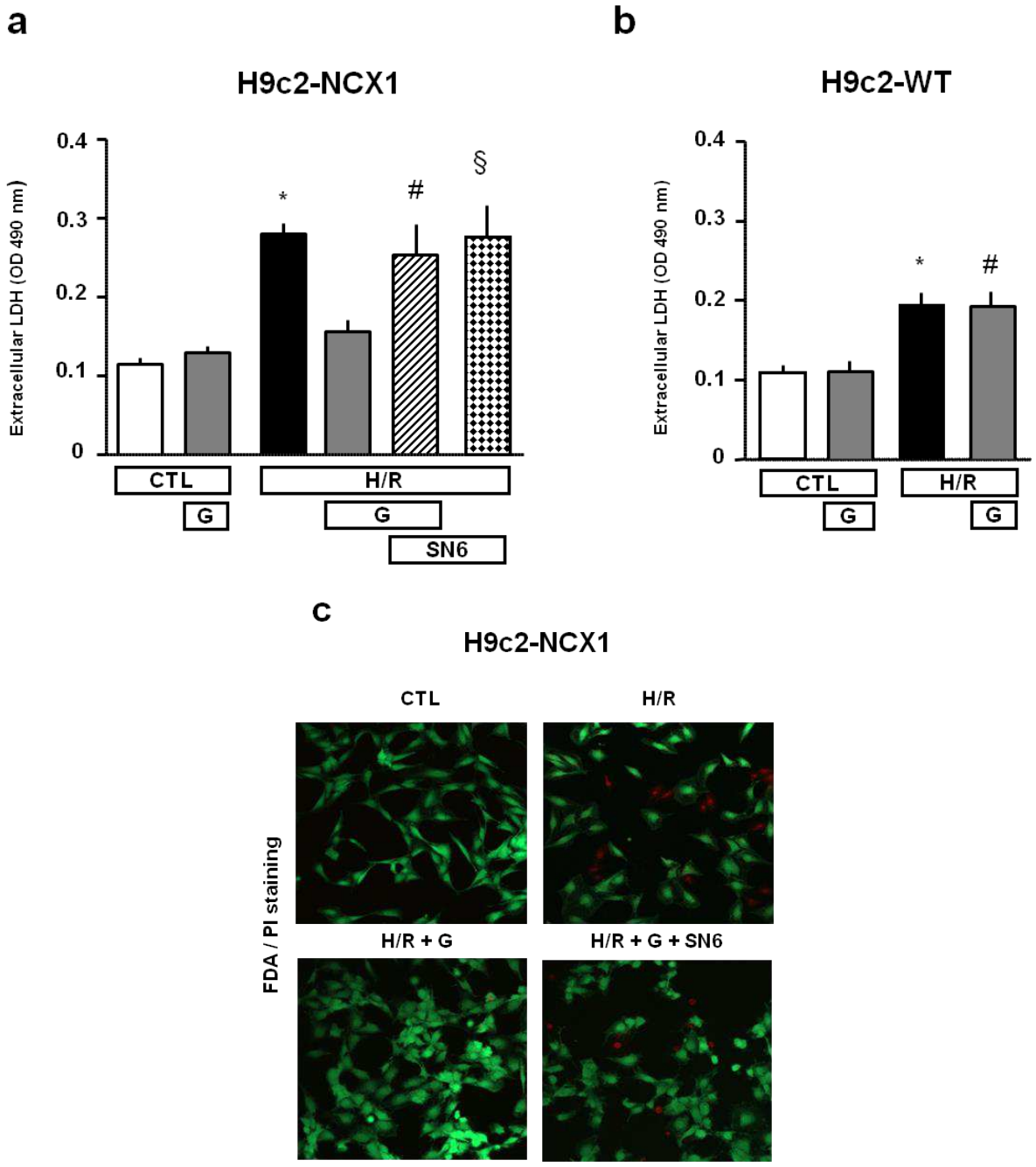

Fig. 3.2: Effect of NCX inhibition on glutamate-induced protection against H/R injury in H9c2. Extracellular LDH activity and FDA/PI double staining measured after the H/R protocol in different experimental conditions. 1 mM glutamate, alone or in combination with 1 μM SN-6, was added during the reoxygenation phase. Differences among means were assessed by one-way ANOVA followed by Dunnet's post hoc test. Each column represents the mean ± S.E.M. of almost 5 independent experiments performed in duplicate. (**a**) *p<0.001 versus CTL, CTL+G and H/R+G; #p<0.001 versus CTL, p<0.01 versus CTL+G and p<0.05 versus H/R +G; §p<0.001 versus CTL and CTL+G, p<0.01 versus H/R +G. (**b**) *p<0.01 versus CTL and CTL+G; #p< 0.001 versus CTL and p<0.01 versus CTL+G.

Noteworthy, the same results were obtained in primary culture of rat adult cardiomyocytes, which endogenously express NCX1. When cardiomyocytes were subjected to the H/R protocol shown in **Fig. 2.2b**, glutamate supplementation at the onset of the reoxigenation greatly reduced H/R-induced cell damage whereas the glutamate-induced protection was lost in the presence of SN-6 (**Fig. 3.3**). In line with results obtained in H9c2-NCX1 cells, SN-6 during the reoxygenation phase had no effect on cell survival, as well as cardiomyocytes viability was not compromised by glutamate when used at 1 mM concentration under normoxic conditions (**Fig. 3.3**).

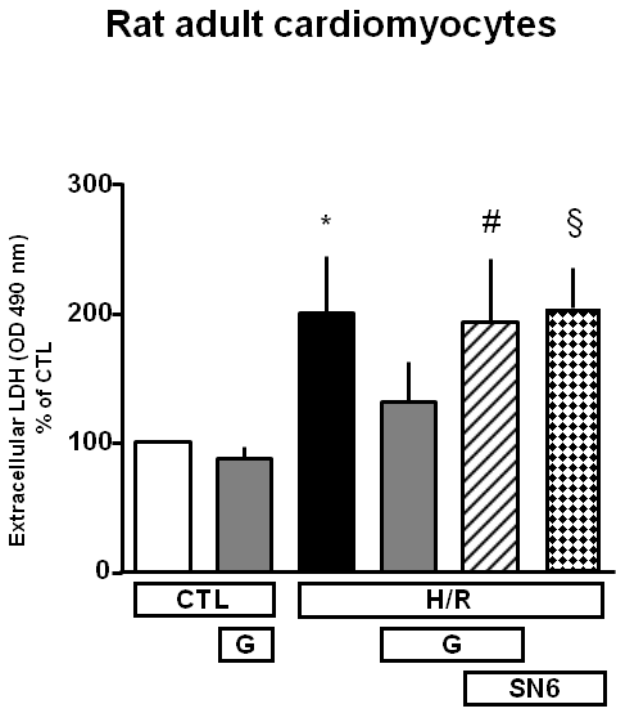

Fig. 3.3: Effect of NCX inhibition on glutamate-induced protection against H/R injury in rat adult cardiomyocytes. Extracellular LDH activity was assessed after the H/R protocol in different experimental conditions. 1 mM glutamate, alone or in combination with 1 μM SN-6, was added during the reoxygenation phase. LDH.levels were and then normalized to the control (normoxia-exposed) group and expressed as percentage. Differences among means were assessed by one-way ANOVA followed by Dunnet's post hoc test.. Each column represents the mean ± S.E.M. of almost 4 independent experiments performed in duplicate. *$p<0.001$ versus CTL and CTL+G and $p<0.05$ versus H/R +G; #$p<0.001$ versus CTL+G, $p<0.01$ versus CTL and $p<0.05$ versus H/R+G; §$p<0.001$ versus CTL and CTL+G, and $p<0.05$ versus H/R and H/R +G. Images are representative of 3 independent experiments.

3.2 Effect of glutamate on H/R injury: involvement of EAATs

It is widely accepted that plasma membrane Excitatory Amino Acid Transporters (EAATs) are primarily responsible for glutamate entry into the cells (King, Lin et al. 2006). It has also been reported that, in particular physiological conditions, glutamate entry into the cells through EAATs relies upon NCX activity (Magi, Arcangeli et al. 2013).

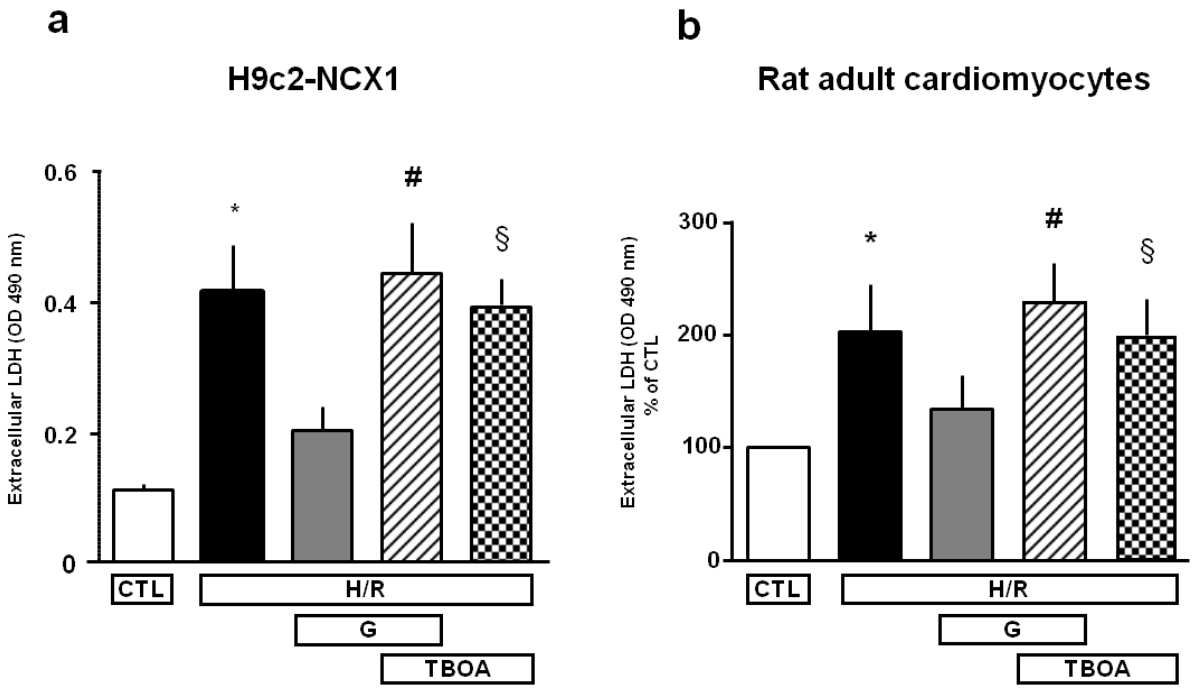

Fig. 3.4: Effect of EAATs inhibition on glutamate-induced protection against H/R injury. Extracellular LDH activity measured 5 h after the hypoxic insult (3 h) in H9c2-NCX1 cells (**a**) and 2 h after the hypoxic insult (1.5 h) in rat adult cardiomyocytes (**b**) in different experimental conditions. 1 mM glutamate, alone or in combination with 300 μM DL-TBOA, was added during the reoxygenation phase. Differences among means were assessed by one-way ANOVA followed by Dunnet's post hoc test. (**a**) Each column represents the mean ± S.E.M. of almost 6 independent experiments performed in triplicate. *$p < 0.001$ versus CTL and $p < 0.01$ versus H/R + G; #$p < 0.001$ versus CTL and $p < 0.01$ versus H/R + G; §$p < 0.001$ versus CTL and $p < 0.01$ versus H/R + G. (**b**) LDH levels were normalized to the control (normoxia-exposed) group and expressed as percentage. Each column represents the mean ± S.E.M. of 4 independent experiments performed in duplicate. *$p < 0.001$ versus control groups and $p < 0.05$ versus H/R + G; #$p < 0.001$ versus control groups and H/R + G; §$p < 0.01$ versus CTL and $p < 0.05$ versus H/R + G.

Thus, once demonstrated that a functional NCX1 was required for glutamate-induced protection against H/R injury, the EAATs involvement in this phenomenon was further explored by using the non-transportable EAATs blocker DL-*threo*-β-Benzyloxyaspartic acid (DL-TBOA), which *per se* does not affect cell viability neither in normoxia (data not shown) nor after H/R (**Fig. 3.4**). H9c2-NCX1 cells were exposed to the H/R protocol in the presence of glutamate and DL-TBOA, used at the concentration of 300 μM, for the entire reoxigenation phase and then cell viability was assessed by LDH. As shown in **Fig. 3.4a** glutamate failed to prevent H/R-induced cell death in the presence of DL-TBOA in H9c2-NCX1 cells. The same results were obtained in primary culture of rat adult cardiomyocytes exposed to the H/R protocol shown in **Fig. 2.1b** (**Fig. 3.4b**). Collectively, these findings support the critical role of EAATs in the observed glutamate-induced protective response.

3.3 Effect of glutamate exposure on ATP production

To better understand the potential mechanism underlying the protective action exerted by glutamate and the specific contribution of NCX1 in such metabolic pathway, the ability of glutamate to enhance ATP production was assessed first in normoxia and then during H/R in H9c2 cells. Since it has been reported that NCX activity supports glutamate-enhanced ATP synthesis in physiological conditions, ATP levels were evaluated during H/R to test whether this pathway could be involved in the recovery of cardiac metabolism from hypoxic state. As shown in **Fig. 3.5** when cells were exposed to different glutamate concentration (0.5 and 1 mM) for 1h, a remarkable increase in ATP synthesis occurred in H9c2-NCX1 but not in H9c2-WT cells in line with previous results (Magi, Arcangeli et al. 2013). Given that H9c2-WT cells were refractory to glutamate

stimulation only H9c2-NCX1 cells were used for the following experiments.

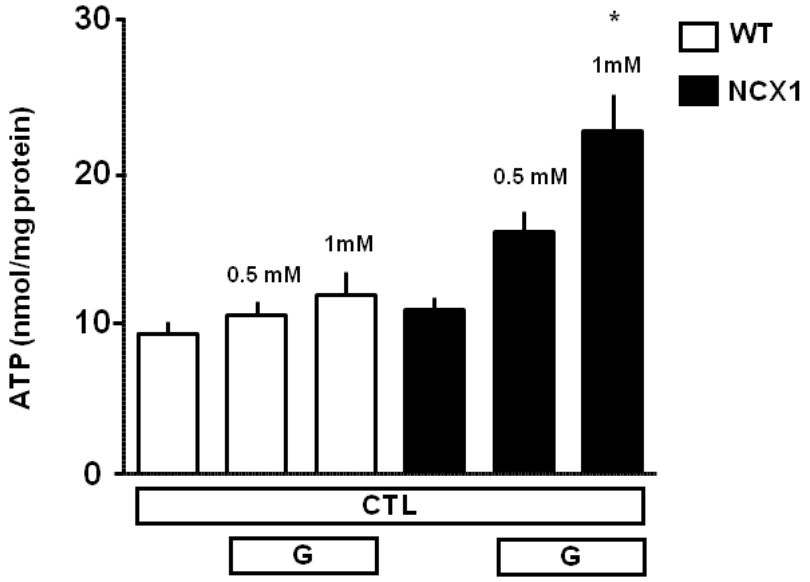

Fig. 3.5: Effect of glutamate exposure on ATP production. Intracellular ATP levels evaluated under normoxic conditions in both H9c2-WT and H9c2-NCX1 cells exposed to different glutamate concentrations (0.5 and 1 mM) for 1h. ATP levels were normalized to the respective sample protein content. Differences among means were assessed by one-way ANOVA followed by Dunnet's post hoc test. Each column represents the mean ± S.E.M. of almost 10 independent experiments performed in triplicate. (a) *$p<0.001$ versus CTL and $p<0.05$ versus 0.5 mM.

To test the ability of glutamate to fuel ATP recovery after hypoxia, glutamate at concentration of 1 mM was added at the onset of the reoxigenation and maintained for one hour. The analyses of intracellular ATP content after the first hour of reoxygenation revealed a significant decline in ATP levels in cells exposed to H/R challenge compared to the control (nmol/mg protein: 5.8±0.3 versus 10.0±0.3) (**Fig. 3.6**). Notewoerthy, glutamate supplementation during the first hour of reoxygenation was able to evoke a raise in ATP production up to the levels observed under normoxic conditions (nmol/mg protein: 11.0±1.1 versus 10.0±0.3) (**Fig. 3.6**).

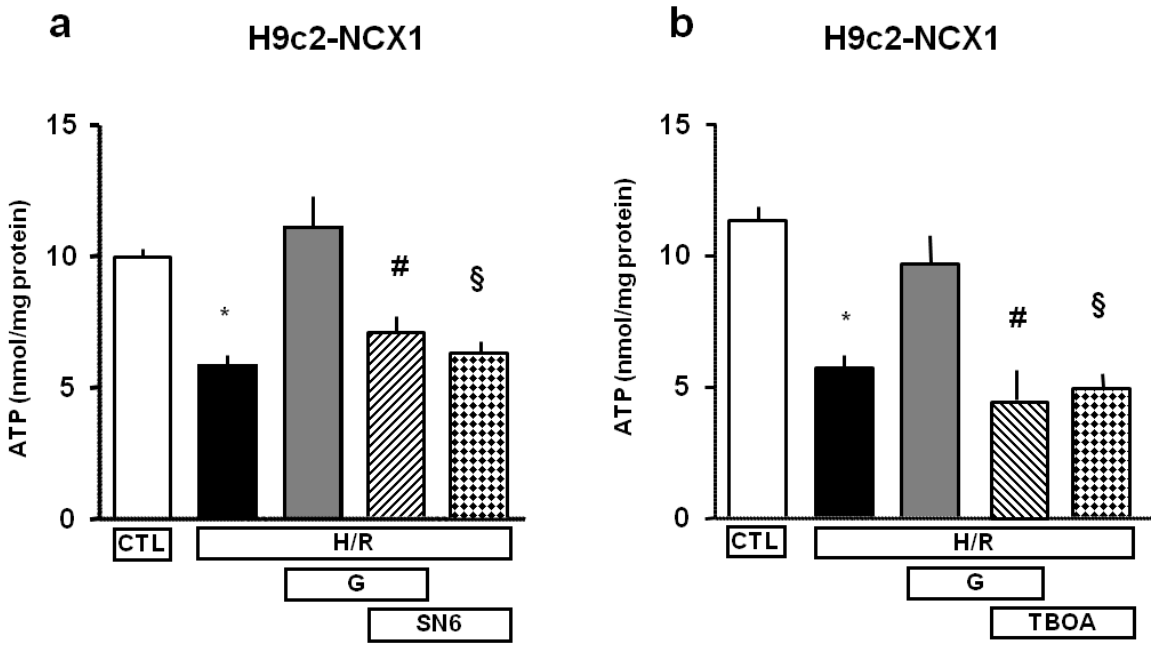

Fig. 3.6: Effect of NCX and EAATs inhibition on glutamate-induced ATP synthesis in H9c2-NCX1 cells subjected to H/R. Intracellular ATP levels evaluated in different experimental conditions. 1 mM glutamate, alone or in combination with 1 μM SN-6 or 300 μM DL-TBOA, was added during the reoxygenation phase, then ATP levels were monitored after 1 h. (**a**) *p<0.001 versus CTL and H/R+G; #p<0.05 versus CTL and p<0.001 versus H/R+G; §p<0.01 versus CTL and p<0.001 versus H/+G. (**b**) *p<0.001 versus CTL and H/R+G; #p<0.001 versus CTL and H/R+G; §p<0.001 versus CTL and H/R+G.

Since the protective effect of glutamate relied both on NCX1 and EAATs (**Figs. 3.2 and 3.4**), which functionally interact to allow glutamate entry into the cell improving its energetic state, to further explore whether the NCX/EAAT functional coupling could play any role in glutamate-enhanced ATP synthesis in H/R setting, the respective inhibitors SN-6 (1 μM) and DL TBOA (300 μM) were added together with glutamate during the reoxigenation. Both SN-6 and DL-TBOA do not affect ATP levels neither in normoxia nor after H/R protocol (**Fig. 3.6a,b**). Interestingly, the ability of glutamate to restore ATP levels was abolished by SN-6 as shown in **Fig. 3.6a** (nmol/mg protein: 11.0±1.1 versus 6.84±0.66), confirming that NCX1 activity is critical for the recovery of oxidative metabolism promoted by glutamate during the reoxigenation. Further,

glutamate ability to restore ATP levels after hypoxia was abolished by DL-TBOA addition (**Fig. 3.6b**) confirming the involvement of EAATs in such glutamate-induced protective response.

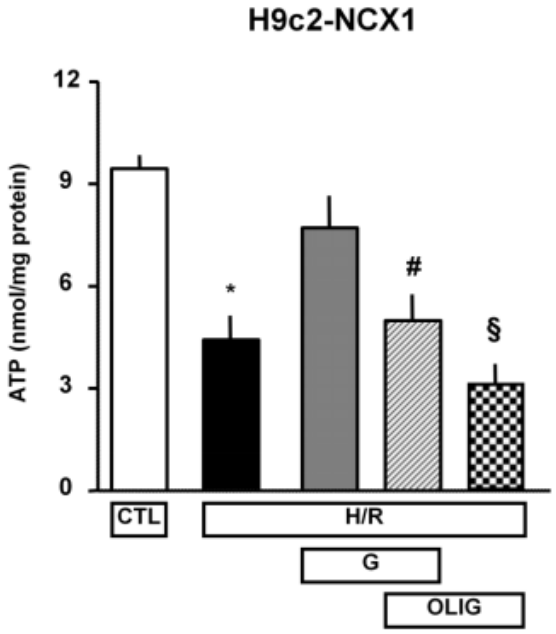

Fig. 3.7: Effect on mitochondrial function of glutamate-induced ATP synthesis in H9c2-NCX1 cells subjected to H/R. Intracellular ATP content evaluated after H/R in the presence of 1 mM glutamate, alone or in combination with 3 µg/ml olygomicin, added at the beginning of the reoxygenation phase and maintained for 1 h. ATP levels were normalized to the respective sample protein content. Differences among means were assessed by one-way ANOVA followed by Dunnet's post hoc test. Each column represents the mean ± S.E.M. of 6 independent experiments performed in triplicate. *p<0.001 versus and H/R+G, #p< 0.001 versus H/R and versus H/R+OLIG and p<0.01 versus H/R+G+OLIG, §p<0.001 versus CTL and H/R+G.

To further confirm the potential mechanism underlying the beneficial effect exerted by glutamate, its ability to enhance ATP production in H9c2-NCX1 cells subjected to H/R was tested in the presence of oligomycin (Magi, Arcangeli et al. 2013), which inhibits ATP synthase by blocking its proton channel (Fo subunit). The inhibition of the oxidative phosphorylation pathway by oligomicin addition during the reoxygenation was able to fully prevent the ATP response to glutamate (**Fig. 3.7**).

3.4 Effect of glutamate on mitochondrial function following H/R challenge

The set of experiments presented here were performed in order to further a) characterize the metabolic response to glutamate in the post-hypoxic phase, b) assess whether glutamate-induced protection could be related to an improvement of oxidative metabolism, c) explore the role of NCX1 in mitochondrial responses to glutamate.

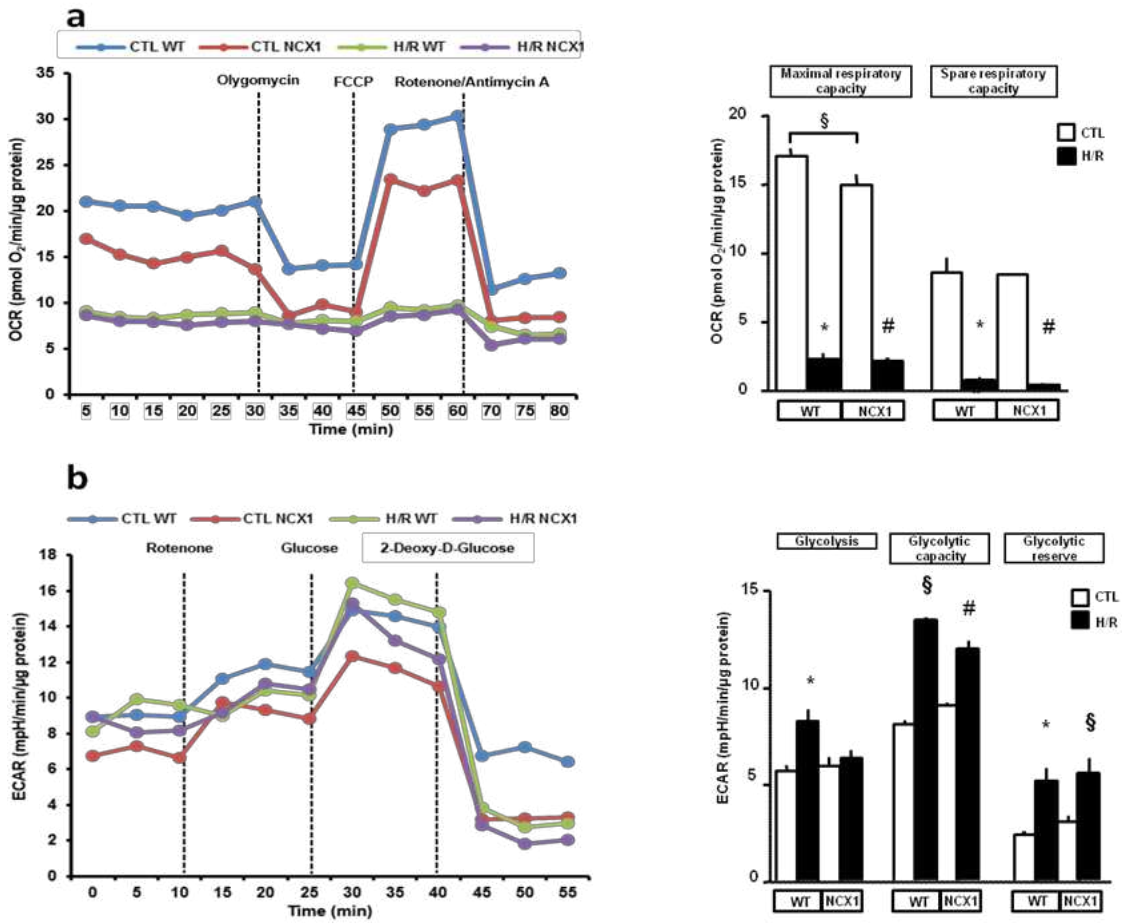

Fig. 3.8: Energy metabolism characterization in H9c2-WT and H9c2-NCX1 cells. Oxidative phosphorylation rate (**a**) and glycolysis rate (**b**) determined by Seahorse XF24 Extracellular Flux Analyzer in H9c2-WT and H9c2-NCX1 cells exposed to 3 h of hypoxia followed by 1 h of reoxygenation. Each column represents the mean ±S.E.M. of 3 replications. Where unseen, error bars overlap with the histogram outline. Differences among means were assessed by Student's t- test. Left panels show representative traces of both OCR and ECAR experiments. Representative profiles of the Seahorse assays are also shown. (**a**) Maximal respiratory capacity: §P<0.05; *p<0.001 and #p<0.001 versus the respective control. Spare respiratory capacity: *p<0.001 and #p<0.001 versus the respective

control. (**b**) Glycolysis: *p<0.01 versus the respective control. Glycolytic capacity: §p<0.001 and p<0.001 versus the respective control. Glycolytic reserve: *p<0.01 and §p<0.01 versus the respective control.

First, the metabolic phenotype of H9c2-WT and H9c2-NCX1 cells was tested by analyzing mitochondrial respiration, assessed as oxygen consumption rate (OCR) and the glycolytic activity, measured as extracellular acidification rate (ECAR) of the surrounding media (which predominately reflects the excretion of lactic acid converted from pyruvate). Experimental operative protocols are summarized in **Figs 2.3** and **2.4** (see "Methods" for further details). In normoxic conditions, ECAR at baseline was not different between H9c2-WT and H9c2-NCX1 cells, whereas maximal respiratory capacity was slightly but significantly smaller in H9c2-NCX1 cells (**Fig. 3.8**). When H/R stress was applied, both cell lines showed a marked decrease in mitochondrial oxygen consumption that was better compensated in H9c2-WT by an increase in glycolysis (**Fig. 3.8**). Next, OCR and ECAR parameters were measured in hypoxic H9c2-NCX1 cells reoxygenated in the presence of glutamate. As shown in **Fig. 3.9a**, after glutamate treatment, OCR profiles greatly improved toward normoxic values. In particular, H9c2-NCX1 cells reoxygenated in the presence of glutamate showed a significant recovery of maximal respiratory capacity, which indicates increased activity of the electron transport chain (ETC), as well as a significant improvement in spare respiratory capacity, which estimates cell's ability to cope with large increases in energy demand and reflects the amount of extra ATP that can be produced by oxidative phosphorylation. Notably, the recovery of OCR profiles induced by glutamate was significantly inhibited when NCX1 was blocked with SN-6 during the reoxygenation phase (**Fig. 3.9a**). Finally, as shown in **Fig. 3.9b**, glycolytic activity was significantly reduced by glutamate supplementation during H/R in H9c2-NCX1 cells, and also this metabolic response was sensitive to NCX1 blockade. Collectively, these data lend further support to the hypothesis that NCX1 is

critical for the glutamate-dependent metabolic boost in myocytes recovering from hypoxic insult, and that the ATP production stimulated by glutamate during the reoxygenation phase essentially relies on mitochondrial oxidative phosphorylation.

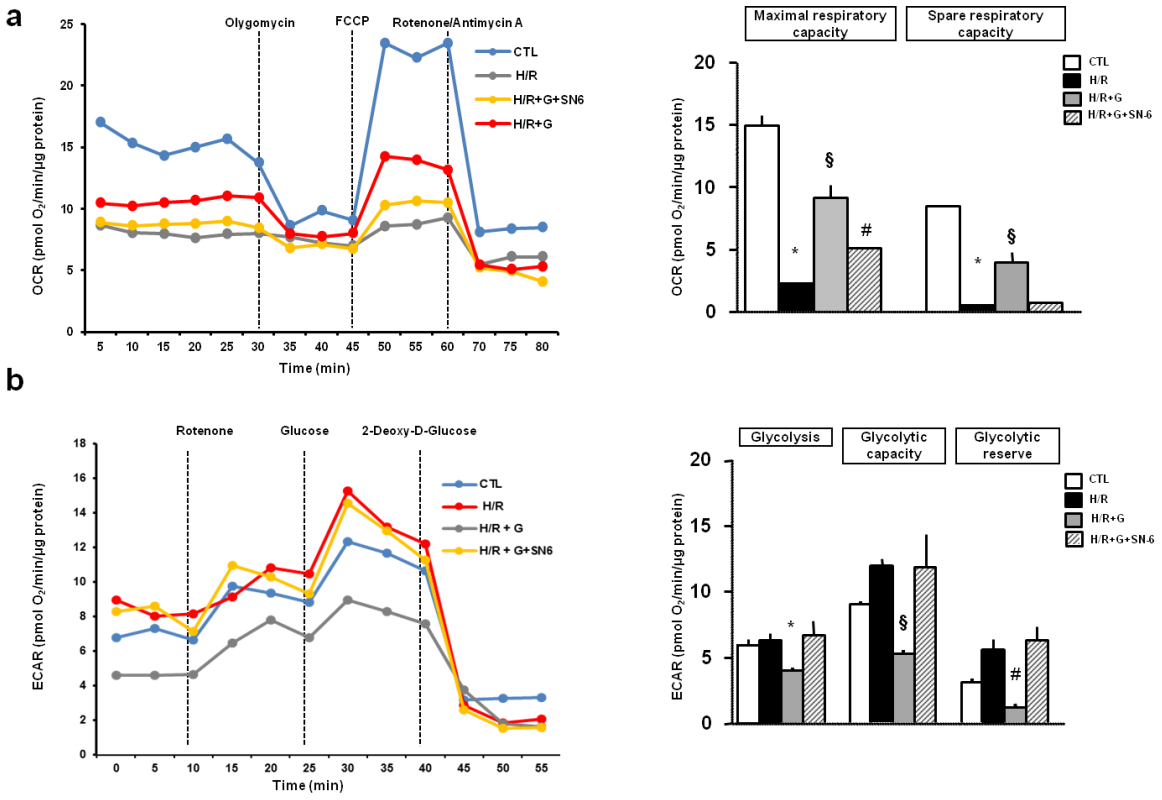

Fig. 3.9: Effect of glutamate supplementation and NCX1 inhibition on cellular metabolism in H9c2-NCX1 cells subjected to H/R challenge. Oxidative phosphorylation rate (**a**) and glycolysis rate (**b**) determined by Seahorse XF24 Extracellular Flux Analyzer in H9c2-NCX1 cells exposed to 3 h of hypoxia followed by 1 h of reoxygenation in different experimental conditions. 1 mM glutamate, alone or in combination with 1 µM SN-6, was added during the reoxygenation phase and maintained for 1 h. Each column represents the mean ± S.E.M. of 4 replications. Where unseen, error bars overlap with the histogram outline. Differences among means were assessed by one-way ANOVA followed by Dunnet's post hoc test. Left panels show representative traces of both OCR and ECAR experiments. (**a**) Maximal respiratory capacity: *p<0.001 versus CTL and H/R+G, p<0.01 versus H/R+G+SN-6; §p<0.001 versus all groups; #p<0.001 versus CTL and H/R+G, p<0.01 versus H/R. Spare respiratory capacity: *p<0.001 versus CTL and H/R+G; §p<0.001 versus all groups. (**b**) Glycolysis: *p<0.05 versus CTL, p<0.01 versus H/R and H/R+g+SN-6. Glycolyitic capacity: §p<0.05 versus CTL, p<0.001 versus H/R and H/R+G+SN-6. Glycolytic reserve: *p<0.01 versus CTL; #p<0.05 versus CTL, p<0.001 versus H/R and H/R+G+SN-6.

3.5 Effect of glutamate exposure on ROS production following H/R challenge

ROS generated during prolonged ischemia and subsequent reperfusion are known to significantly contribute to H/R injury. In particular, during reoxygenation the molecular oxygen reintroduced to hypoxic myocytes can be converted to oxygen free radicals above viable levels (Li and Jackson 2002). To test whether the protective effect of glutamate could also rely on its ability to prevent ROS-induced cell death, ROS levels were monitored in H9c2 cells after H/R protocol (**Fig. 2.9a**). As shown in **Fig. 3.10**, H/R injury was found to increase markedly ROS production in H9c2-NCX1 cells and that glutamate was able to partially, but significantly, reduced such increase.

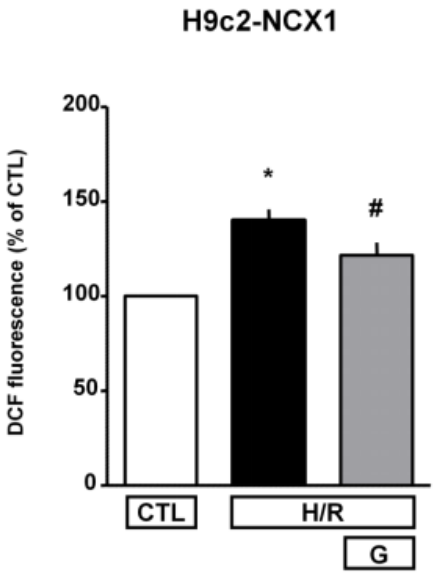

Fig. 3.10: Effect of glutamate exposure on ROS production in H9c2-NCX1 cells subjected to H/R. Intracellular ROS production assessed after H/R challenge by evaluation of the DCF fluorescence in the presence of 1 mM glutamate during the reoxygenation phase. DCF fluorescence values were normalized to untreated control and expressed as percentage. Differences among means were assessed by one-way ANOVA followed by Dunnet's post hoc test. Each column represents the mean ± S.E.M. of almost 6 independent experiments performed in triplicate. *$p<0.001$ versus CTL and $p<0.05$ versus H/R+G.

3.6 Analysis of NCX 1 and EAATs expression following H/R challenge

Previous studies showed that both in different cardiac models NCX1 protein expression is upregulated under stressful conditions, including hypertrophy and ischemic injury (Castaldo, Macri et al. 2016). In line with previous reports, here protein expression analysis revealed that NCX1 levels were increased after H/R in H9c2-NCX1 cells whereas in H9c2-WT cells NCX1 protein expression was undetectable both in normoxia and after H/R challenge (**Fig. 3.11**). Since the protective effect of glutamate against H/R damage relied both on NCX1 and EAATs activities, the EAATs expression was also evaluated to test whether it could be modified by H/R challenge. The expression of the three main EAATs expressed in H9c2 cells, namely EAAC1, GLAST and GLT-1 was unmodified after H/R challenge, in both H9c2-WT and H9c2-NCX1 cells (**Fig. 3.12**).

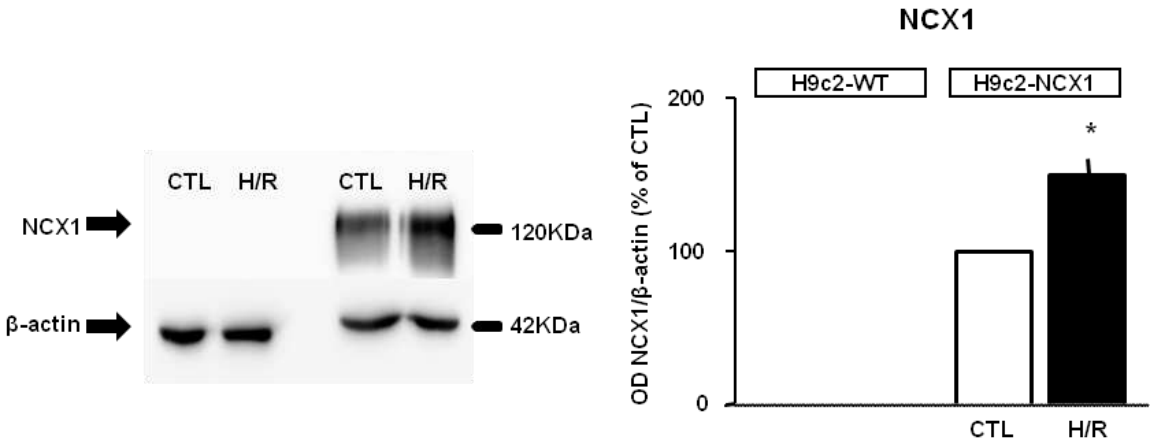

Figure 3.11: NCX1 expression in H9c2-WT and H9c2-NCX1 cells subjected to H/R challenge. Quantitative densitometry showing the expression of NCX in H9c2-WT and H9c2-NCX1 cells exposed to H/R. β-actin was used as loading control. Normalized optical density values are expressed as percentage of the respective control. Each column represents the mean ±S.E.M. of 3 independent experiments. Differences among means were assessed by Student's *t-test*. *p<0.01 versus CTL. Representative western blot images are shown below.

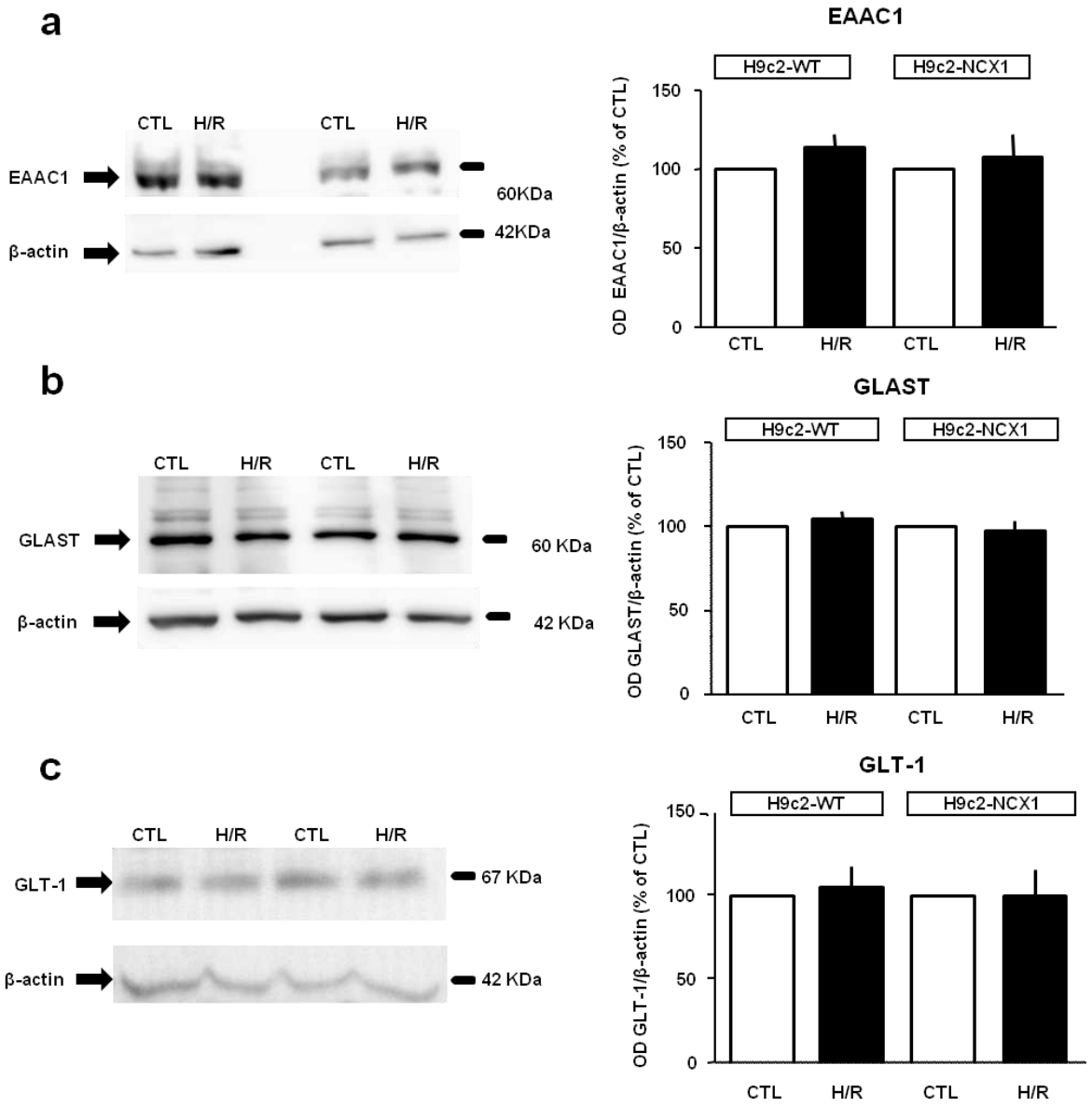

Figure 3.12: EAATs expression in H9c2-WT and H9c2-NCX1 cells subjected to H/R challenge. Quantitative densitometry showing the expression of the Na^+-dependent glutamate transporters EAAC1 (**a**), GLAST (**b**) and GLT-1 (**c**) in H9c2-WT and H9c2-NCX1 cells exposed to H/R. β-actin was used as loading control. Normalized optical density values are expressed as percentage of the respective control. Each column represents the mean ±S.E.M. of 3 independent experiments. Differences among means were assessed by Student's *t-test*. (**a**) *p<0.01 versus CTL. Representative western blot images are shown below.

3.7 Effect of glutamate on NCX1 activity alteration following H/R

The increase in NCX expression observed during cardiac ischemia is often associated to an altered exchanger activity, which contribute to further exacerbate I/R-induced cell damage by promoting intracellular Ca^{2+} overload (Castaldo, Macri et al. 2016). To test whether glutamate-induced protection might involve the normalization of NCX1 function, the exchanger activity was monitored in H9c2-NCX1 exposed to H/R. Cells loaded with the calcium indicator Fluo-4 AM were subjected to isotonic extracellular Na^+ removal at the end of the experimental of H/R protocol reported in **Fig. 2.2a** (see "Methods" for further details). No change in fluorescence baseline was observed in H9c2-WT cells subjected to the same Na^+ removal protocol (data not shown), confirming that the Ca^{2+} responses observed in H9c2-NCX1 are mediated by NCX1 reverse mode.

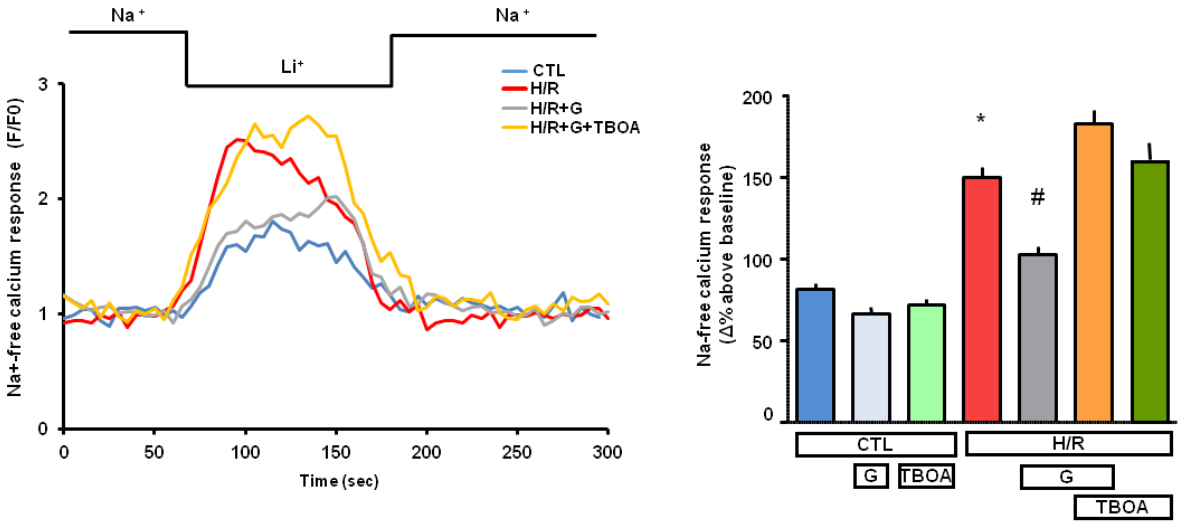

Fig 3.13: Effect of EAATs inhibition on glutamate exposure on NCX activity in H9c2-NCX1 cells subjected to H/R. On the left representative records of Ca^{2+} responses to Na^+-free challenge after incubation in normoxic conditions (blu line), H/R insult (red line), and after H/R challenge in the presence of 1 mM glutamate during the entire reoxygenation phase alone (grey line) and in combination with 300 µM DL-TBOA (yellow line). On the right bar graph showing the analysis of the reverse mode of NCX1 activity in the presence of 1 mM glutamate alone or in combination with 300 µM DL-TBOA in normoxic and hypoxic conditions. Differences among means were assessed by one-way ANOVA followed by Dunnet's *post hoc* test. The bar plot reports

the mean ± S.E.M. of the $[Ca^{2+}]_i$ increase elicited by Na^+-free pulse. For each experimental group, 100-200 cells were recorded in different experimental sessions. *p<0.001 versus all groups except than versus H/R+ TBOA and HR+G+TBOA (not significant); # p<0.01 versus all groups except than versus all control groups. For fluorescence intensity and Δ% calculation see Methods (2.9.1) for further details.

As shown in **Figs. 3.13** and **3.14**, when NCX1 reverse mode was activated by superfusing a Na^+-free extracellular solution, in control cells a rise in intracellular Ca^{2+} concentration of about 80% occurred, as revealed by the increase in fluorescence signal. When H/R group was analyzed, the NCX1-mediated increase in $[Ca^{2+}]_i$ was enhanced (about 50%) compared to what observed in control cells. When glutamate was added during the entire reoxygenation phase, NCX1 reverse activity was normalized to normoxic values and was significantly reduced compared to H/R group. Glutamate failed to prevent the rise in intracellular calcium occurred during H/R in the presence of both DL- TBOA and SN-6, which do not affect *per s*e calcium responses, neither in normoxia nor in H/R conditions.

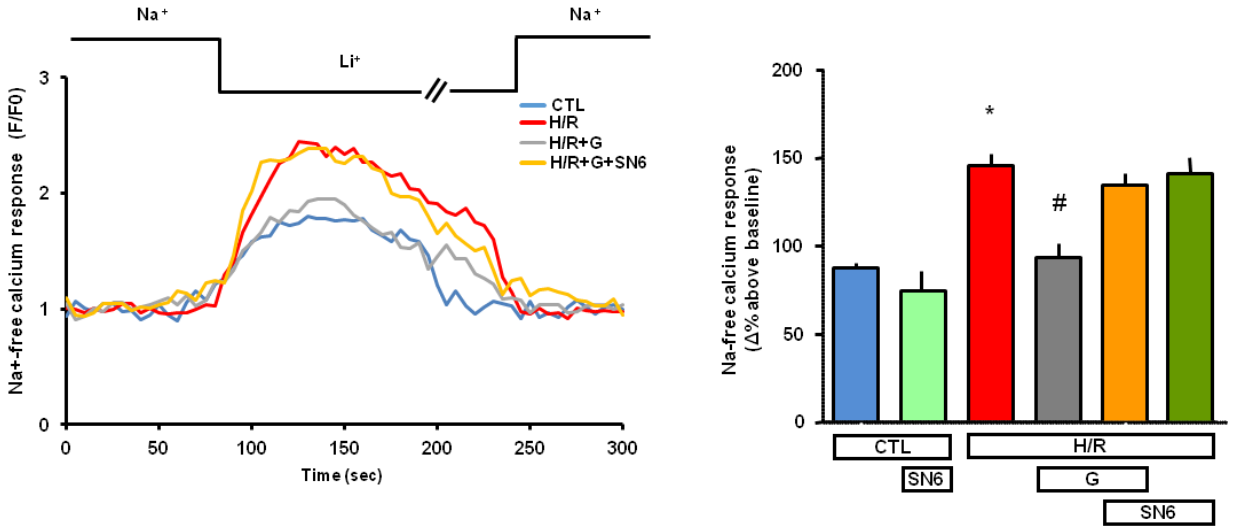

Fig 3.14: Effect of NCX inhibition on glutamate exposure on NCX activity in H9c2-NCX1 cells subjected to H/R. On the left representative records of Ca^{2+} responses to Na^+-free challenge after incubation in normoxic conditions (blu line), H/R insult (red line), and after H/R challenge in the presence of 1 mM glutamate during the entire reoxygenation phase alone (grey line) and in combination with 1 μM SN-6 (yellow line). On the right bar graph showing the analysis of the reverse mode of NCX1 activity in the presence of 1 mM glutamate alone or in combination with 1 μM SN-6 in normoxic and

hypoxic conditions. Differences among means were assessed by one-way ANOVA followed by Dunnet's *post hoc* test. The bar plot reports the mean ± S.E.M. of the $[Ca^{2+}]_i$ increase elicited by Na^+-free pulse. For each experimental group, 100-200 cells were recorded in different experimental sessions. *$p<0.001$ versus all groups except than versus H/R+ SN-6 and H/R+G+SN-6 (not significant); # $p<0.01$ versus all groups except than versus all control groups (not significant). For fluorescence intensity and Δ% calculation (see Methods **2.9.1** for further details).

4. DISCUSSION

4.1 Rationale

Disorders characterized by I/R, such as myocardial infarction, stroke, and peripheral vascular disease, continue to be among the most frequent causes of disease and death (Ferrer Gracia, Hernandez-Antolin et al. 2007). Discoveries reported over the past 30 years have been focused to thoroughly understand the underlying mechanisms of I/R injury with the hope for developing therapies to limit the devastating health and economic burdens imposed by disorders characterized by reductions in organ-specific blood flow. Recent findings supporting the concept that reperfusion could "per se" induce and exacerbate tissue injury induced by ischemia provided a major impetus for research because this component of damage is manageable to therapeutic intervention. Thus, physicians and biomedical researchers have recently turned their attention towards therapeutic approaches that target the multiple pathologic processes occurring during reperfusion to limit I/R injury and/or enhance resistance to cell death (Kalogeris, Baines et al. 2012). In particular, interventions in the area of metabolic substrate enhancement have been reported to improve post-ischemic recovery reducing consistently the extent of the tissue injury. However, the effects of ischemia on metabolic substrate preference has not been fully appreciated yet: oxygen deprivation during ischemia will significantly alter the relative ability of the heart to utilize different sources of energy. Amino acids are of particular interest in this regard due to their potential for non-oxidative metabolism and their low contribution to cellular acidification (Drake, 2012). The rationale for the use of glutamate in this study was to provide an anaplerotic substrate which can be easily metabolized when oxygen is reintroduced to the ischemic tissue. Glutamate in the heart is one of the main constituent of the free intracellular amino acid pool but also a key metabolite of myocardial energy metabolism. It can be used as intermediate of the Krebs cycle and enhance ATP production improving the energetic state of the cells. During

myocardial ischemia, glutamate levels diminish and therefore high exogenous concentrations of glutamate are required to compensate this loss (Drake, Sidorov et al. 2012). Indeed, clinical and experimental evidence has demonstrated that glutamate-induced cardioprotection requires glutamate supplementation in the millimolar range (Williams, King et al. 2001, Kristiansen, Lofgren et al. 2008, Lofgren, Povlsen et al. 2010). At the concentration used of 1 mM, which is somehow higher than basal plasma levels, glutamate has no evident toxic effect on H9c2 cells and rat adult cardiomyocytes. Further, ATP synthesis in H9c2-NCX1 cells was significantly enhanced when glutamate was used at 1 mM concentration (**Fig. 3.5**) in line with previous results (Magi, Lariccia et al. 2012).

4.2 Glutamate counteracts H/R-induced injury in cardiac cells by sustaining ATP production in a NCX1 dependent manner.

Overall, the data obtained from this report provide clear evidence that glutamate supplementation during the reoxygenation phase counteracted H/R-induced injury in cardiac cells and that NCX1 displays a key role in such protective response. The mechanism underlying this glutamate-induced cardioprotection has been showed being related to its ability to boost energetic metabolism by sustaining ATP production and closely linked to the presence of NCX1 to enhance cell viability in cardiac models of H/R. Indeed, the data obtained clearly showed that glutamate was able to sustain mitochondrial ATP synthesis thereby promote cell survival in H9c2-NCX1 (expressing NCX1) but not in H9c2-WT (not expressing NCX1) exposed to H/R. Further evidence that a functional NCX1 is determinant for glutamate protection was obtained in H9c2-NCX1 by pharmacological blockade of NCX1 with SN-6 1 μM. The addition of the inhibitor at the onset of the reoxygenation phase completely prevented the beneficial effects of glutamate in terms of recovery of ATP synthesis (**Fig. 3.6a**) and mitochondrial respiration (**Fig. 3.9**),

cell protection (**Fig. 3.2**) and normalization of Na^+/Ca^{2+}exchanger activity (**Fig. 3.14**). The crucial role exerted by NCX1 was also supported in a different cardiac model of rat adult caridomyocytes, where glutamate failed to improve cell viability against H/R injury when NCX1 was inhibited (**Fig. 3.3**). Interestingly, SN-6 applied at the concentration of 1 μM only during the reoxygenation phase failed to protect H9c2-NCX1 cells or rat adult cardiomyocytes against H/R injury, in line with previous data obtained in different cell lines expressing NCX1 (Castaldo, Macri et al. 2016). Although it has been reported that pharmacological blockade of NCX1 throughout the entire H/R protocol may provide cardioprotection by restricting excessive Ca^{2+} accumulation via inhibition of the reverse mode operation of NCX in different cardiac models (Chen and Li 2012), an excessive reduction in exchanger activity is also expected to be deleterious because of massive perturbation of calcium homeostasis since NCX1 is the primary mechanism of Ca^{2+} extrusion from the cardiomyocyte) (Jordan, Henderson et al. 2010) It's role in cardiac ischemia has been described for many years as detrimental. However, a beneficial action it has been recently disclosed for NCX1 in promoting cardioprotection induced by preconditioning. (Castaldo, Macri et al. 2016). Moreover, here for the first time it has been revealed a key role of NCX1 in the glutamate cardioprotection against H/R-induced cell injury.

Over the years alternative experimental interventions aimed to improve cardiac metabolism against I/R challenge have been considered as potential therapeutic strategies. Available knowledge suggests that glutamate may play a key role for the regulation of mitochondrial function in relation to I/R injury. Since glutamate is taken up in larger quantities by the ischemic than by the non-ischemic stressed human heart (Mudge et al. 1976; Thomassen et al. 1988), its use as an additive to cardioplegic solutions during cardiac surgery has been shown a cardioprotective effect (Pereda et al. 2007). Indeed, rat hearts perfused with high glutamate concentrations during reperfusion displays a decreased infarct size (Kristiansen et al. 2008).

In line with these reports, we found that glutamate supplementation from the start of the reoxygenation phase dramatically improved cell viability in our cardiac models of H/R (**Figs 3.2 and 3.3**). Since the resumption of aerobic metabolism is an important step in the recovery of cardiac cells upon reperfusion, the effect of glutamate supplementation on ATP production and the involvement of NCX1 in such metabolic response has been deeply investigated both in physiological and pathological conditions. As shown in **Fig. 3.5,** in physiological conditions glutamate was able to enhance ATP synthesis only in the presence of a functional NCX1. Meanwhile, when H9c2-NCX1 cells were subjected to H/R challenge, ATP levels were dramatically reduced and completely counteracted by glutamate exposure during the first hour of reoxigenation (**Fig. 3.6**). The key role of NCX1 in the glutamate-induced ATP synthesis was confirmed by the use of NCX1 inhibitor SN-6 (**Fig. 3.5a**).

4.3 Glutamate counteracts H/R-induced injury in cardiac cells by sustaining ATP production in an EAATs dependent manner

According to several studies, glutamate-induced ischemic cardioprotection might depend on amino acid transamination during reperfusion and activity of the malate–aspartate shuttle (Lofgren, Povlsen et al. 2010), which is the main metabolic cycle for transfer of reduced equivalents from the cytosolic to the intramitochondrial compartment for oxidation (Safer, 1975). The shuttle activity is regulated by substrate availability and specific mitochondrial aspartate/glutamate carrier proteins (Contreras et al. 2007), and includes coupled mitochondrial and cytosolic transamination of glutamate and aspartate to α- ketoglutarate and oxaloacetate. However, there is an alternative pathway, whereby a member of the EAATs family EAAC1 and NCX1 cooperate in order to favor glutamate entry into the cytoplasm and then into the mitochondria, stimulating ATP synthesis (Magi, Lariccia et al. 2012,

Magi, Arcangeli et al. 2013). Thus, the reverse mode of NCX activity allows glutamate entry into the cells through EAAC1 leading to an increase in cytosolic [Ca^{2+}], which in turn can be buffered by mitochondria stimulating Ca^{2+}-dependent dehydrogenases of the respiratory chain and hence ATP supply under conditions of increased ATP demand (Denton 2009). The involvement of EAATs in such metabolic pathway was tested in the presence of the non-transportable EAATs inhibitor DL-TBOA (300 μM). As expected, the ability of glutamate to stimulate ATP recovery (**Fig. 3.6**) and restore cell viability (**Fig. 3.4**) was fully abolished by DL-TBOA addition, confirming that glutamate entrance into the cells was mediated by EAATs. At mitochondrial level glutamate can be used as metabolic fuel for mitochondrial ATP synthesis, and in this process, Ca^{2+} signals originated by the reversed NCX activity can also play a role.

4.4 Glutamate-induced normalization of NCX1 activity during H/R relies on EAATs/NCX1 dependent pathway

Since NCX1 expression was found increased after H/R both in the heart (Castaldo, Macri et al. 2016) and in H9c2-NCX1 cells (**Fig. 3.12**), the activity of the exchanger was also monitored to test whether intracellular Ca^{2+} levels might be involved in the glutamate-induced cardioprotection. The experiments performed with the fluorescent Ca^{2+} indicator Fluo-4 showed an increase of NCX1 reverse mode in cells subjected to H/R that was partially abolished when cells were reoxygenated in the presence of 1 mM glutamate, which failed to normalize the echanger activity in the presence of both DL-TBOA (**Fig. 3.13**) and SN-6 (**Fig. 3.14**). The glutamate-induced ATP response observed in H/R cells may contribute to promote cell survival by sustaining the activity of the ATPase-dependent transporters which in turn may contribute to restore intracellular Na^+ and Ca^{2+} levels limiting calcium overload. According to a different theory, this increased ATP content in the presence of Ca^{2+} transients

may evoke the formation of membrane domains that spontaneously vesiculate to the cytoplasmic side inducing a rapid massive endocytosis, which may remove NCX1 from the cell surface, thereby limiting its activity (Lariccia, Fine et al. 2011).

4.5 Glutamate-enhanced ATP response during H/R relies on an improved mitochondrial oxidative phosporylation

Glutamate ability to promote ATP production by oxidative phosphorilation was also supported by the capacity of oligomycin to fully prevent the glutamate-induced ATP response during the reoxigenation (**Fig. 3.7**). Further, the detailed analyses of ECAR and OCR parameters both in normoxic and hypoxic conditions in H9c2-WT and H9c2-NCX1 cells has revealed additional information on the mechanism underlying the glutamate-induced protection. Hypoxic H9c2-NCX1 cells showed a marked decrease in mitochondrial activity that was better compensated by an increase in glycolisis in H9c2-WT cells. However, H9c2-NCX1 reoxigenated in the presence of glutamate showed a recovery of OCR profiles, which revealed an improved activity of ETC determinant to sustain the increased ATP demand during reoxygenation phase (**Fig. 3.9a**) that was accompanied to a decline in glycolitic activity (**Fig. 3.9b**). The glutamate-induced decrease of glycolytic rate observed in H/R H9c2-NCX1 cells may also contribute to the cardioprotection by limiting the amount of acidic products (i.e. lactate) and proton accumulation that account for a quantitatively significant proportion of I/R-induced cell damage (Kalogeris, Baines et al. 2012). The drop in glycolisis as well as the improvement of mitochondrial activity induced by glutamate in H/R was significantly suppressed when NCX1 was blocked with SN-6, further highlighting the key role of this exchanger in glutamate-dependent protection of ischemic myocytes. Thus, these data lend further support to the hypothesis that the glutamate-induced ATP response essentially relies on mitochondrial

oxidative phosporylation. During reoxygenation the molecular oxygen reintroduced to hypoxic myocytes can be converted to oxygen free radicals above viable levels, and glutamate can improve the reducing power of myocytes. Indeed, the increase in ROS levels observed during H/R in H9c2-NCX1 cells was partially prevented by glutamate supplementation (**Fig. 3.10**). ROS generation under pathophysiological conditions in which Complex I is inhibited or damaged, such as I/R, is regulated by the rate of NADH generation/oxidation in the mitochondrial matrix. In the presence of glutamate, the rate of ROS production is closely related to local NADH generation. When glutamate is metabolized, NADH generated by the tricarboxylic acid (TCA) cycle is rapidly oxidized to maintain a low $NADH/NAD^+$ ratio which in turn may contribute to inhibit ROS production (Korge, Ping et al. 2008). Indeed, the preservation of free radical scavengers and the restoration of energetic metabolism may act as synergistic components of glutamate-induced protection.

4.6 Conclusion

Collectively these data disclosed a new beneficial and essential role of NCX1 in glutamate-induced cell survival in cardiac models of H/R sustaining that glutamate supplementation from the beginning of the reoxygenation phase reduced the H/R-mediated energy impairment that leads to cell death by enhancing oxidative metabolism, with a clear involvement of the EAATs/NCX pathway (Maiolino, Castaldo et al. 2017).

This conclusion is supported by the following evidence:

- in H9c2 cells, glutamate productively sustained mitochondrial ATP synthesis thereby promoting survival in H9c2-NCX1 (expressing NCX1) but not in H9c2-WT (not expressing NCX1) (**Figs. 3.1 and 3.2**);
- in H9c2-NCX1 cells, pharmacological blockade of NCX1 and EAATs during the

reoxygenation phase completely prevented the beneficial effects of glutamate in terms of recovery of ATP synthesis (**Fig. 3.6**) and mitochondrial respiration (**Fig. 3.7**), cell protection (**Figs. 3.3 and 3.4**) and normalization of NCX activity (**Figs. 3.13 and 3.14**);

- in rat adult cardiomyocytes, glutamate failed to protect cells against H/R injury when NCX1 was inhibited at the reoxigenation (**Fig. 3.3**).

In particular, as for normoxic conditions, EAATs activity might stimulate NCX1 reverse mode of operation, leading to an increase in the mitochondrial Ca2+, which plays a crucial role as promoting survival factor in such glutamate-induced protective response. Indeed, the increase of the reverse mode of NCX1 develops within seconds and relies on the presence of extracellular glutamate that, being cotransported with Na^+ into the cell via EAATs, influences both Na^+ gradient across plasma membrane and membrane potential (Magi, Arcangeli et al. 2013). Overall, these results provide clear evidence that glutamate supplementation from the beginning of the reoxygenation phase can positively affect cell viability by sustaining the oxidative metabolism and increasing the rate of ATP content, with NCX1 and EAATs playing a crucial role. In this scenario, there must be a critical point representing the boundary between cytoprotective and cytotoxic effects related to the increase in intracellular Ca^{2+}, and this point might critically rely upon NCX1 activity. Indeed, on one hand Ca^{2+} may promote cell survival by stimulating mitochondrial Ca2+-sensitive dehydrogenase activity and energy production, on the other hand it may be toxic and trigger either apoptotic or necrotic death pathways (Orrenius, Zhivotovsky et al. 2003). Thus, NCX1 activity helping to fine tune Ca^{2+} influx and efflux from cells might be crucial in unrevealing its dual role as survival factor or devious killer in living organisms.

5. BIBLIOGRAPHY

Anselmi, A., A. Abbate, F. Girola, G. Nasso, G. G. Biondi-Zoccai, G. Possati and M. Gaudino (2004). "Myocardial ischemia, stunning, inflammation, and apoptosis during cardiac surgery: a review of evidence." Eur J Cardiothorac Surg **25**(3): 304-311.

Aronsen, J. M., F. Swift and O. M. Sejersted (2013). "Cardiac sodium transport and excitation-contraction coupling." J Mol Cell Cardiol **61**: 11-19.

Baetz, D., M. Bernard, C. Pinet, S. Tamareille, S. Chattou, H. El Banani, A. Coulombe and D. Feuvray (2003). "Different pathways for sodium entry in cardiac cells during ischemia and early reperfusion." Mol Cell Biochem **242**(1-2): 115-120.

Bers, D. M. (2008). "Calcium cycling and signaling in cardiac myocytes." Annu Rev Physiol **70**: 23-49.

Blaustein, M. P. and W. J. Lederer (1999). "Sodium/calcium exchange: its physiological implications." Physiol Rev **79**(3): 763-854.

Bulkley, G. B. (1987). "Free radical-mediated reperfusion injury: a selective review." Br J Cancer Suppl **8**: 66-73.

Carafoli, E. (1987). "Intracellular calcium homeostasis." Annu Rev Biochem **56**: 395-433.

Carafoli, E. (1988). "The intracellular homeostasis of calcium: an overview." Ann N Y Acad Sci **551**: 147-157; discussion 157-148.

Casey, T. M., P. G. Arthur and M. A. Bogoyevitch (2007). "Necrotic death without mitochondrial dysfunction-delayed death of cardiac myocytes following oxidative stress." Biochim Biophys Acta **1773**(3): 342-351.

Castaldo, P., M. L. Macri, V. Lariccia, A. Matteucci, M. Maiolino, S. Gratteri, S. Amoroso and S. Magi (2016). "Na+/Ca2+ exchanger 1 inhibition abolishes ischemic tolerance induced by ischemic preconditioning in different cardiac models." Eur J Pharmacol **794**: 246-256.

Chen, S. and S. Li (2012). "The Na+/Ca(2)+ exchanger in cardiac ischemia/reperfusion injury." Med Sci Monit **18**(11): RA161-165.

Cohen, M. V. and J. M. Downey (1996). "Myocardial preconditioning promises to be a novel approach to the treatment of ischemic heart disease." Annu Rev Med **47**: 21-29.

Croall, D. E. and K. Ersfeld (2007). "The calpains: modular designs and functional diversity." Genome Biol **8**(6): 218.

de Servi, S., E. Poma and G. Specchia (1988). "[Coronary spasm and vasoconstriction in the pathogenesis of acute myocardial ischemia]." Rev Esp Cardiol **41**(9): 511-516.

de Windt, L. J., K. Cox, L. Hofstra and P. A. Doevendans (2002). "Molecular and genetic aspects of cardiac fatty acid homeostasis in health and disease." Eur Heart J **23**(10): 774-787.

Denton, R. M. (2009). "Regulation of mitochondrial dehydrogenases by calcium ions." Biochim Biophys Acta **1787**(11): 1309-1316.

Diaz, M. E., S. C. O'Neill and D. A. Eisner (2004). "Sarcoplasmic reticulum calcium content fluctuation is the key to cardiac alternans." Circ Res **94**(5): 650-656.

Drake, K. J., V. Y. Sidorov, O. P. McGuinness, D. H. Wasserman and J. P. Wikswo (2012). "Amino acids as metabolic substrates during cardiac ischemia." Exp Biol Med (Maywood) **237**(12): 1369-1378.

Emery, L., S. Whelan, K. D. Hirschi and J. K. Pittman (2012). "Protein Phylogenetic Analysis of Ca(2+)/cation Antiporters and Insights into their Evolution in Plants." Front Plant Sci **3**: 1.

Ferguson, T. B., Jr., P. K. Smith, G. K. Lofland, W. L. Holman, M. A. Helms and J. L. Cox (1986). "The effects of cardioplegic potassium concentration and myocardial temperature on electrical activity in the heart during elective cardioplegic arrest." J Thorac Cardiovasc Surg **92**(4): 755-765.

Ferrer Gracia, M. C., R. A. Hernandez-Antolin, M. J. Perez-Vizcayno, C. Conde Vela, F. Alfonso Manterola and C. Macaya Miguel (2007). "[Myocardial infarction with ST segment elevation and angiographically normal coronary arteries: epidemiology and mid-term follow-up]." Med Clin (Barc) **129**(18): 694-696.
Frank, A., M. Bonney, S. Bonney, L. Weitzel, M. Koeppen and T. Eckle (2012). "Myocardial ischemia reperfusion injury: from basic science to clinical bedside." Semin Cardiothorac Vasc Anesth **16**(3): 123-132.
Garcia-Dorado, D., A. Rodriguez-Sinovas, M. Ruiz-Meana and J. Inserte (2014). "Protection against myocardial ischemia-reperfusion injury in clinical practice." Rev Esp Cardiol (Engl Ed) **67**(5): 394-404.
Garcia-Dorado, D., M. Ruiz-Meana and H. M. Piper (2009). "Lethal reperfusion injury in acute myocardial infarction: facts and unresolved issues." Cardiovasc Res **83**(2): 165-168.
Genda, E. N., J. G. Jackson, A. L. Sheldon, S. F. Locke, T. M. Greco, J. C. O'Donnell, L. A. Spruce, R. Xiao, W. Guo, M. Putt, S. Seeholzer, H. Ischiropoulos and M. B. Robinson "Co-compartmentalization of the astroglial glutamate transporter, GLT-1, with glycolytic enzymes and mitochondria." J Neurosci **31**(50): 18275-18288.
Genda, E. N., J. G. Jackson, A. L. Sheldon, S. F. Locke, T. M. Greco, J. C. O'Donnell, L. A. Spruce, R. Xiao, W. Guo, M. Putt, S. Seeholzer, H. Ischiropoulos and M. B. Robinson (2011). "Co-compartmentalization of the astroglial glutamate transporter, GLT-1, with glycolytic enzymes and mitochondria." J Neurosci **31**(50): 18275-18288.
Gerczuk, P. Z. and R. A. Kloner (2012). "An update on cardioprotection: a review of the latest adjunctive therapies to limit myocardial infarction size in clinical trials." J Am Coll Cardiol **59**(11): 969-978.
Giladi, M., S. Y. Lee, Y. Ariely, Y. Teldan, R. Granit, R. Strulovich, Y. Haitin, K. Y. Chung and D. Khananshvili (2017). "Structure-based dynamic arrays in regulatory domains of sodium-calcium exchanger (NCX) isoforms." Sci Rep **7**(1): 993.
Giladi, M., R. Shor, M. Lisnyansky and D. Khananshvili (2016). "Structure-Functional Basis of Ion Transport in Sodium-Calcium Exchanger (NCX) Proteins." Int J Mol Sci **17**(11).
Goodwin, G. W. and H. Taegtmeyer (2000). "Improved energy homeostasis of the heart in the metabolic state of exercise." Am J Physiol Heart Circ Physiol **279**(4): H1490-1501.
Groenke, S., E. D. Larson, S. Alber, R. Zhang, S. T. Lamp, X. Ren, H. Nakano, M. C. Jordan, H. S. Karagueuzian, K. P. Roos, A. Nakano, C. Proenza, K. D. Philipson and J. I. Goldhaber (2013). "Complete atrial-specific knockout of sodium-calcium exchange eliminates sinoatrial node pacemaker activity." PLoS One **8**(11): e81633.
Hattori, Y., N. Matsuda, J. Kimura, T. Ishitani, A. Tamada, S. Gando, O. Kemmotsu and M. Kanno (2000). "Diminished function and expression of the cardiac Na+-Ca2+ exchanger in diabetic rats: implication in Ca2+ overload." J Physiol **527 Pt 1**: 85-94.
Healy, D. A., I. Feeley, C. J. Keogh, T. G. Scanlon, P. A. Hodnett, A. G. Stack, M. Clarke Moloney, P. Whittaker and S. R. Walsh (2015). "Remote ischemic conditioning and renal function after contrast-enhanced CT scan: A randomized trial." Clin Invest Med **38**(3): E110-118.
Herlitz, J., M. Dellborg, T. Karlsson, M. H. Evander, A. Berger and R. Luepker (2008). "Epidemiology of acute myocardial infarction with the emphasis on patients who did not reach the coronary care unit and non-AMI admissions." Int J Cardiol **128**(3): 342-349.
Huang, Y., M. Zhou, H. Sun and Y. Wang (2011). "Branched-chain amino acid metabolism in heart disease: an epiphenomenon or a real culprit?" Cardiovasc Res **90**(2): 220-223.
Imahashi, K., C. Pott, J. I. Goldhaber, C. Steenbergen, K. D. Philipson and E. Murphy (2005). "Cardiac-specific ablation of the Na+-Ca2+ exchanger confers protection against ischemia/reperfusion injury." Circ Res **97**(9): 916-921.

Jeffs, G. J., B. P. Meloni, A. J. Bakker and N. W. Knuckey (2007). "The role of the Na(+)/Ca(2+) exchanger (NCX) in neurons following ischaemia." J Clin Neurosci **14**(6): 507-514.
Jordan, M. C., S. A. Henderson, T. Han, M. C. Fishbein, K. D. Philipson and K. P. Roos (2010). "Myocardial function with reduced expression of the sodium-calcium exchanger." J Card Fail **16**(9): 786-796.
Kalogeris, T., C. P. Baines, M. Krenz and R. J. Korthuis (2012). "Cell biology of ischemia/reperfusion injury." Int Rev Cell Mol Biol **298**: 229-317.
Kanemoto, S., M. Matsubara, M. Noma, B. G. Leshnower, L. M. Parish, B. M. Jackson, R. Hinmon, H. Hamamoto, J. H. Gorman, 3rd and R. C. Gorman (2009). "Mild hypothermia to limit myocardial ischemia-reperfusion injury: importance of timing." Ann Thorac Surg **87**(1): 157-163.
Karlsson, R. M., K. Tanaka, L. M. Saksida, T. J. Bussey, M. Heilig and A. Holmes (2009). "Assessment of glutamate transporter GLAST (EAAT1)-deficient mice for phenotypes relevant to the negative and executive/cognitive symptoms of schizophrenia." Neuropsychopharmacology **34**(6): 1578-1589.
Khanna, S., R. Stewart, S. Gnyawali, H. Harris, M. Balch, J. Spieldenner, C. K. Sen and C. Rink (2017). "Phytoestrogen isoflavone intervention to engage the neuroprotective effect of glutamate oxaloacetate transaminase against stroke." FASEB J **31**(10): 4533-4544.
King, N., H. Lin, J. D. McGivan and M. S. Suleiman (2006). "Expression and activity of the glutamate transporter EAAT2 in cardiac hypertrophy: implications for ischaemia reperfusion injury." Pflugers Arch **452**(6): 674-682.
Kirischuk, S., H. Kettenmann and A. Verkhratsky (2007). "Membrane currents and cytoplasmic sodium transients generated by glutamate transport in Bergmann glial cells." Pflugers Arch **454**(2): 245-252.
Kolwicz, S. C., Jr., S. Purohit and R. Tian (2013). "Cardiac metabolism and its interactions with contraction, growth, and survival of cardiomyocytes." Circ Res **113**(5): 603-616.
Korge, P., P. Ping and J. N. Weiss (2008). "Reactive oxygen species production in energized cardiac mitochondria during hypoxia/reoxygenation: modulation by nitric oxide." Circ Res **103**(8): 873-880.
Kristiansen, S. B., B. Lofgren, N. B. Stottrup, H. H. Kimose, J. E. Nielsen-Kudsk, H. E. Botker and T. T. Nielsen (2008). "Cardioprotection by L-glutamate during postischaemic reperfusion: reduced infarct size and enhanced glycogen resynthesis in a rat insulin-free heart model." Clin Exp Pharmacol Physiol **35**(8): 884-888.
Kristiansen, S. B., J. E. Nielsen-Kudsk, H. E. Botker and T. T. Nielsen (2005). "Effects of KATP channel modulation on myocardial glycogen content, lactate, and amino acids in nonischemic and ischemic rat hearts." J Cardiovasc Pharmacol **45**(5): 456-461.
Lariccia, V., M. Fine, S. Magi, M. J. Lin, A. Yaradanakul, M. C. Llaguno and D. W. Hilgemann (2011). "Massive calcium-activated endocytosis without involvement of classical endocytic proteins." J Gen Physiol **137**(1): 111-132.
Lejay, A., F. Fang, R. John, J. A. Van, M. Barr, F. Thaveau, N. Chakfe, B. Geny and J. W. Scholey (2015). "Ischemia reperfusion injury, ischemic conditioning and diabetes mellitus." J Mol Cell Cardiol.
Levy, J. H. and K. A. Tanaka (2003). "Inflammatory response to cardiopulmonary bypass." Ann Thorac Surg **75**(2): S715-720.
Li, C. and R. M. Jackson (2002). "Reactive species mechanisms of cellular hypoxia-reoxygenation injury." Am J Physiol Cell Physiol **282**(2): C227-241.
Lofgren, B., J. A. Povlsen, L. E. Rasmussen, N. B. Stottrup, L. Solskov, P. M. Krarup, S. B. Kristiansen, H. E. Botker and T. T. Nielsen (2010). "Amino acid transamination is crucial for ischaemic cardioprotection in normal and preconditioned isolated rat hearts--focus on L-glutamate." Exp Physiol **95**(1): 140-152.

Lopaschuk, G. D. (2017). "Metabolic Modulators in Heart Disease: Past, Present, and Future." Can J Cardiol **33**(7): 838-849.
Lopaschuk, G. D. and J. R. Ussher (2017). "Evolving Concepts of Myocardial Energy Metabolism: More Than Just Fats and Carbohydrates." Circ Res **119**(11): 1173-1176.
Lytton, J. (2007). "Na+/Ca2+ exchangers: three mammalian gene families control Ca2+ transport." Biochem J **406**(3): 365-382.
Ma, L., B. Zhu, X. Chen, J. Liu, Y. Guan and J. Ren (2008). "Abnormalities of sarcoplasmic reticulum Ca2+ mobilization in aortic smooth muscle cells from streptozotocin-induced diabetic rats." Clin Exp Pharmacol Physiol **35**(5-6): 568-573.
Magi, S., S. Arcangeli, P. Castaldo, A. A. Nasti, L. Berrino, E. Piegari, R. Bernardini, S. Amoroso and V. Lariccia (2013). "Glutamate-induced ATP synthesis: relationship between plasma membrane Na+/Ca2+ exchanger and excitatory amino acid transporters in brain and heart cell models." Mol Pharmacol **84**(4): 603-614.
Magi, S., V. Lariccia, P. Castaldo, S. Arcangeli, A. A. Nasti, A. Giordano and S. Amoroso (2012). "Physical and functional interaction of NCX1 and EAAC1 transporters leading to glutamate-enhanced ATP production in brain mitochondria." PLoS One **7**(3): e34015.
Maiolino, M., P. Castaldo, V. Lariccia, S. Piccirillo, S. Amoroso and S. Magi (2017). "Essential role of the Na(+)-Ca2(+) exchanger (NCX) in glutamate-enhanced cell survival in cardiac cells exposed to hypoxia/reoxygenation." Sci Rep **7**(1): 13073.
Matsuoka, S., D. A. Nicoll, L. V. Hryshko, D. O. Levitsky, J. N. Weiss and K. D. Philipson (1995). "Regulation of the cardiac Na(+)-Ca2+ exchanger by Ca2+. Mutational analysis of the Ca(2+)-binding domain." J Gen Physiol **105**(3): 403-420.
Maus, A. and G. J. Peters (2016). "Glutamate and alpha-ketoglutarate: key players in glioma metabolism." Amino Acids **49**(1): 21-32.
McCommis, K. S., Z. Chen, X. Fu, W. G. McDonald, J. R. Colca, R. F. Kletzien, S. C. Burgess and B. N. Finck (2015). "Loss of Mitochondrial Pyruvate Carrier 2 in the Liver Leads to Defects in Gluconeogenesis and Compensation via Pyruvate-Alanine Cycling." Cell Metab **22**(4): 682-694.
McCommis, K. S. and B. N. Finck (2015). "Mitochondrial pyruvate transport: a historical perspective and future research directions." Biochem J **466**(3): 443-454.
Merchant, S., S. Nadaraj, D. Chowdhury, V. A. Parnell, C. Sison, E. J. Miller and K. Ojamaa (2008). "Macrophage migration inhibitory factor in pediatric patients undergoing surgery for congenital heart repair." Mol Med **14**(3-4): 124-130.
Molinaro, P., O. Cuomo, G. Pignataro, F. Boscia, R. Sirabella, A. Pannaccione, A. Secondo, A. Scorziello, A. Adornetto, R. Gala, D. Viggiano, S. Sokolow, A. Herchuelz, S. Schurmans, G. Di Renzo and L. Annunziato (2008). "Targeted disruption of Na+/Ca2+ exchanger 3 (NCX3) gene leads to a worsening of ischemic brain damage." J Neurosci **28**(5): 1179-1184.
Molinaro, P., A. Pannaccione, M. J. Sisalli, A. Secondo, O. Cuomo, R. Sirabella, M. Cantile, R. Ciccone, A. Scorziello, G. di Renzo and L. Annunziato (2015). "A new cell-penetrating peptide that blocks the autoinhibitory XIP domain of NCX1 and enhances antiporter activity." Mol Ther **23**(3): 465-476.
Mukhopadhyay, S., M. Saqcena and D. A. Foster (2015). "Synthetic lethality in KRas-driven cancer cells created by glutamine deprivation." Oncoscience **2**(10): 807-808.
Murphy, E. and D. G. Allen (2009). "Why did the NHE inhibitor clinical trials fail?" J Mol Cell Cardiol **46**(2): 137-141.
Murry, C. E., R. B. Jennings and K. A. Reimer (1986). "Preconditioning with ischemia: a delay of lethal cell injury in ischemic myocardium." Circulation **74**(5): 1124-1136.
Netticadan, T., R. Temsah, M. Osada and N. S. Dhalla (1999). "Status of Ca2+/calmodulin protein kinase phosphorylation of cardiac SR proteins in ischemia-reperfusion." Am J Physiol **277**(3 Pt 1): C384-391.

Netticadan, T., R. M. Temsah, K. Kawabata and N. S. Dhalla (2000). "Sarcoplasmic reticulum Ca(2+)/Calmodulin-dependent protein kinase is altered in heart failure." Circ Res **86**(5): 596-605.
Nielsen, T. T., N. B. Stottrup, B. Lofgren and H. E. Botker (2011). "Metabolic fingerprint of ischaemic cardioprotection: importance of the malate-aspartate shuttle." Cardiovasc Res **91**(3): 382-391.
Niu, C. F., Y. Watanabe, K. Ono, T. Iwamoto, K. Yamashita, H. Satoh, T. Urushida, H. Hayashi and J. Kimura (2007). "Characterization of SN-6, a novel Na+/Ca2+ exchange inhibitor in guinea pig cardiac ventricular myocytes." Eur J Pharmacol **573**(1-3): 161-169.
O'Connell, T. D., M. C. Rodrigo and P. C. Simpson (2007). "Isolation and culture of adult mouse cardiac myocytes." Methods Mol Biol **357**: 271-296.
Orrenius, S., B. Zhivotovsky and P. Nicotera (2003). "Regulation of cell death: the calcium-apoptosis link." Nat Rev Mol Cell Biol **4**(7): 552-565.
Paradis, S., A. L. Charles, A. Meyer, A. Lejay, J. W. Scholey, N. Chakfe, J. Zoll and B. Geny (2016). "Chronology of mitochondrial and cellular events during skeletal muscle ischemia-reperfusion." Am J Physiol Cell Physiol **310**(11): C968-982.
Perrelli, M. G., P. Pagliaro and C. Penna (2011). "Ischemia/reperfusion injury and cardioprotective mechanisms: Role of mitochondria and reactive oxygen species." World J Cardiol **3**(6): 186-200.
Peuhkurinen, K. J., T. E. Takala, E. M. Nuutinen and I. E. Hassinen (1983). "Tricarboxylic acid cycle metabolites during ischemia in isolated perfused rat heart." Am J Physiol **244**(2): H281-288.
Philipson, K. D. and D. A. Nicoll (2000). "Sodium-calcium exchange: a molecular perspective." Annu Rev Physiol **62**: 111-133.
Raivio, P., R. Lassila and J. Petaja (2009). "Thrombin in myocardial ischemia-reperfusion during cardiac surgery." Ann Thorac Surg **88**(1): 318-325.
Ralphe, J. C., J. L. Segar, B. C. Schutte and T. D. Scholz (2004). "Localization and function of the brain excitatory amino acid transporter type 1 in cardiac mitochondria." J Mol Cell Cardiol **37**(1): 33-41.
Ren, X. and K. D. Philipson (2013). "The topology of the cardiac Na(+)/Ca(2)(+) exchanger, NCX1." J Mol Cell Cardiol **57**: 68-71.
Rink, C., S. Gnyawali, R. Stewart, S. Teplitsky, H. Harris, S. Roy, C. K. Sen and S. Khanna (2017). "Glutamate oxaloacetate transaminase enables anaplerotic refilling of TCA cycle intermediates in stroke-affected brain." FASEB J **31**(4): 1709-1718.
Roger, V. L. (2007). "Epidemiology of myocardial infarction." Med Clin North Am **91**(4): 537-552; ix.
Rose, E. M., J. C. Koo, J. E. Antflick, S. M. Ahmed, S. Angers and D. R. Hampson (2009). "Glutamate transporter coupling to Na,K-ATPase." J Neurosci **29**(25): 8143-8155.
Salas, M. A., C. A. Valverde, G. Sanchez, M. Said, J. S. Rodriguez, E. L. Portiansky, M. A. Kaetzel, J. R. Dedman, P. Donoso, E. G. Kranias and A. Mattiazzi (2010). "The signalling pathway of CaMKII-mediated apoptosis and necrosis in the ischemia/reperfusion injury." J Mol Cell Cardiol **48**(6): 1298-1306.
Sanada, S., I. Komuro and M. Kitakaze (2011). "Pathophysiology of myocardial reperfusion injury: preconditioning, postconditioning, and translational aspects of protective measures." Am J Physiol Heart Circ Physiol **301**(5): H1723-1741.
Schaper, J., E. Meiser and G. Stammler (1985). "Ultrastructural morphometric analysis of myocardium from dogs, rats, hamsters, mice, and from human hearts." Circ Res **56**(3): 377-391.
Schousboe, A., S. Scafidi, L. K. Bak, H. S. Waagepetersen and M. C. McKenna (2014). "Glutamate metabolism in the brain focusing on astrocytes." Adv Neurobiol **11**: 13-30.

Sheikh, A. Q., J. R. Hurley, W. Huang, T. Taghian, A. Kogan, H. Cho, Y. Wang and D. A. Narmoneva (2012). "Diabetes alters intracellular calcium transients in cardiac endothelial cells." PLoS One **7**(5): e36840.
Shenoda, B. (2015). "The role of Na+/Ca2+ exchanger subtypes in neuronal ischemic injury." Transl Stroke Res **6**(3): 181-190.
Shigeri, Y., R. P. Seal and K. Shimamoto (2004). "Molecular pharmacology of glutamate transporters, EAATs and VGLUTs." Brain Res Brain Res Rev **45**(3): 250-265.
Sisalli, M. J., A. Secondo, A. Esposito, V. Valsecchi, C. Savoia, G. F. Di Renzo, L. Annunziato and A. Scorziello (2014). "Endoplasmic reticulum refilling and mitochondrial calcium extrusion promoted in neurons by NCX1 and NCX3 in ischemic preconditioning are determinant for neuroprotection." Cell Death Differ **21**(7): 1142-1149.
Smith, B. K., C. G. Perry, T. R. Koves, D. C. Wright, J. C. Smith, P. D. Neufer, D. M. Muoio and G. P. Holloway (2012). "Identification of a novel malonyl-CoA IC(50) for CPT-I: implications for predicting in vivo fatty acid oxidation rates." Biochem J **448**(1): 13-20.
Stanley, W. C. (2004). "Myocardial energy metabolism during ischemia and the mechanisms of metabolic therapies." J Cardiovasc Pharmacol Ther **9 Suppl 1**: S31-45.
Svedjeholm, R., I. Vanhanen, E. Hakanson, P. O. Joachimsson, L. Jorfeldt and L. Nilsson (1996). "Metabolic and hemodynamic effects of intravenous glutamate infusion early after coronary operations." J Thorac Cardiovasc Surg **112**(6): 1468-1477.
Taegtmeyer, H. (1994). "Energy metabolism of the heart: from basic concepts to clinical applications." Curr Probl Cardiol **19**(2): 59-113.
Taegtmeyer, H., M. B. Peterson, V. V. Ragavan, A. G. Ferguson and M. Lesch (1977). "De novo alanine synthesis in isolated oxygen-deprived rabbit myocardium." J Biol Chem **252**(14): 5010-5018.
Tal, I., T. Kozlovsky, D. Brisker, M. Giladi and D. Khananshvili (2016). "Kinetic and equilibrium properties of regulatory Ca(2+)-binding domains in sodium-calcium exchangers 2 and 3." Cell Calcium **59**(4): 181-188.
Talukder, M. A., J. L. Zweier and M. Periasamy (2009). "Targeting calcium transport in ischaemic heart disease." Cardiovasc Res **84**(3): 345-352.
Taqueti, V. R. and P. M. Ridker (2013). "Inflammation, coronary flow reserve, and microvascular dysfunction: moving beyond cardiac syndrome X." JACC Cardiovasc Imaging **6**(6): 668-671.
Tepavcevic, S., D. V. Milutinovic, D. Macut, M. Stojiljkovic, M. Nikolic, I. Bozic-Antic, T. Culafic, J. Bjekic-Macut, G. Matic and G. Koricanac (2015). "Cardiac fatty acid uptake and metabolism in the rat model of polycystic ovary syndrome." Endocrine **50**(1): 193-201.
Thurneysen, T., D. A. Nicoll, K. D. Philipson and H. Porzig (2002). "Sodium/calcium exchanger subtypes NCX1, NCX2 and NCX3 show cell-specific expression in rat hippocampus cultures." Brain Res Mol Brain Res **107**(2): 145-156.
Tompkins, A. J., L. S. Burwell, S. B. Digerness, C. Zaragoza, W. L. Holman and P. S. Brookes (2006). "Mitochondrial dysfunction in cardiac ischemia-reperfusion injury: ROS from complex I, without inhibition." Biochim Biophys Acta **1762**(2): 223-231.
Tzingounis, A. V. and J. I. Wadiche (2007). "Glutamate transporters: confining runaway excitation by shaping synaptic transmission." Nat Rev Neurosci **8**(12): 935-947.
Vandenberg, R. J. and R. M. Ryan (2013). "Mechanisms of glutamate transport." Physiol Rev **93**(4): 1621-1657.
Verburg, E., R. M. Murphy, I. Richard and G. D. Lamb (2009). "Involvement of calpains in Ca2+-induced disruption of excitation-contraction coupling in mammalian skeletal muscle fibers." Am J Physiol Cell Physiol **296**(5): C1115-1122.
Vinten-Johansen, J. and W. Shi (2011). "Perconditioning and postconditioning: current knowledge, knowledge gaps, barriers to adoption, and future directions." J Cardiovasc Pharmacol Ther **16**(3-4): 260-266.

Wang, C., H. Chen, J. Zhang, Y. Hong, X. Ding and W. Ying (2014). "Malate-aspartate shuttle mediates the intracellular ATP levels, antioxidation capacity and survival of differentiated PC12 cells." Int J Physiol Pathophysiol Pharmacol **6**(2): 109-114.
Weber, C. R., V. Piacentino, 3rd, S. R. Houser and D. M. Bers (2003). "Dynamic regulation of sodium/calcium exchange function in human heart failure." Circulation **108**(18): 2224-2229.
Weisel, R. D. (1993). "Myocardial stunning after coronary bypass surgery." J Card Surg **8**(2 Suppl): 242-244.
Williams, H., N. King, E. J. Griffiths and M. S. Suleiman (2001). "Glutamate-loading stimulates metabolic flux and improves cell recovery following chemical hypoxia in isolated cardiomyocytes." J Mol Cell Cardiol **33**(12): 2109-2119.
Wilmsdorff, M. V., C. Blaich, M. Zink, J. Treutlein, M. Bauer, T. Schulze, T. Schneider-Axmann, O. Gruber, M. Rietschel, A. Schmitt and P. Falkai (2013). "Gene expression of glutamate transporters SLC1A1, SLC1A3 and SLC1A6 in the cerebellar subregions of elderly schizophrenia patients and effects of antipsychotic treatment." World J Biol Psychiatry **14**(7): 490-499.
Wischmeyer, P. E., D. Jayakar, U. Williams, K. D. Singleton, J. Riehm, E. A. Bacha, V. Jeevanandam, U. Christians and N. Serkova (2003). "Single dose of glutamine enhances myocardial tissue metabolism, glutathione content, and improves myocardial function after ischemia-reperfusion injury." JPEN J Parenter Enteral Nutr **27**(6): 396-403.
Yamashita, J., S. Kita, T. Iwamoto, M. Ogata, M. Takaoka, N. Tazawa, M. Nishikawa, K. Wakimoto, M. Shigekawa, I. Komuro and Y. Matsumura (2003). "Attenuation of ischemia/reperfusion-induced renal injury in mice deficient in Na+/Ca2+ exchanger." J Pharmacol Exp Ther **304**(1): 284-293.
Yang, D., R. Jia and G. Ding (2013). "Selective inhibition of the reverse mode of Na(+)/Ca(2+) exchanger attenuates contrast-induced cell injury." Am J Nephrol **37**(3): 264-273.
Yang, D., R. Jia and J. Tan (2013). "Na+/Ca2+ exchange inhibitor, KB-R7943, attenuates contrast-induced acute kidney injury." J Nephrol **26**(5): 877-885.
Young, V. R. and A. M. Ajami (2000). "Glutamate: an amino acid of particular distinction." J Nutr **130**(4S Suppl): 892S-900S.
Yu, Q., C. F. Lee, W. Wang, G. Karamanlidis, J. Kuroda, S. Matsushima, J. Sadoshima and R. Tian (2014). "Elimination of NADPH oxidase activity promotes reductive stress and sensitizes the heart to ischemic injury." J Am Heart Assoc **3**(1): e000555.
Zhang, J. Y., K. Cheng, D. Lai, L. H. Kong, M. Shen, F. Yi, B. Liu, F. Wu and J. J. Zhou (2015). "Cardiac sodium/calcium exchanger preconditioning promotes anti-arrhythmic and cardioprotective effects through mitochondrial calcium-activated potassium channel." Int J Clin Exp Pathol **8**(9): 10239-10249.
Zhou, Y. and N. C. Danbolt (2014). "Glutamate as a neurotransmitter in the healthy brain." J Neural Transm (Vienna) **121**(8): 799-817.
Zorov, D. B., M. Juhaszova and S. J. Sollott (2006). "Mitochondrial ROS-induced ROS release: an update and review." Biochim Biophys Acta **1757**(5-6): 509-517.